UPPSALA
UNIVERSITET

Digital Comprehensive Summaries of Uppsala Dissertations from the Faculty of Pharmacy 15

Spray-Dried Powders for Inhalation

Particle Formation and Formulation Concepts

JESSICA ELVERSSON

ACTA
UNIVERSITATIS
UPSALIENSIS
UPPSALA
2005

ISSN 1651-6192
ISBN 91-554-6322-3
urn:nbn:se:uu:diva-5904

Dissertation presented at Uppsala University to be publicly examined in B22, BMC, Uppsala, Friday, September 23, 2005 at 09:15 for the degree of Doctor of Philosophy (Faculty of Pharmacy). The examination will be conducted in English.

Abstract
Elversson, J. 2005. Spray-Dried Powders for Inhalation. Particle Formation and Formulation Concepts. Acta Universitatis Upsaliensis. *Digital Comprehensive Summaries of Uppsala Dissertations from the Faculty of Pharmacy* 15. 78 pp. Uppsala. ISBN 91-554-6322-3.

Spray drying is a method with a high potential in the preparation of protein particles suitable for pulmonary delivery. However, surface induced denaturation of bio-molecules during atomization and subsequent drying can be substantial and it is therefore important to develop new formulation concept for concurrent encapsulation and stabilization of proteins during spray drying. Hence, with an overall objective to increase the knowledge of the formation of particulate systems for systemic administration of proteins by spray drying, the first part of this thesis, systematically investigated the particle formation by droplet size and particle size measurements. It was described how specific properties, such as the solubility and the crystallization propensity of the solute, can affect the product, e.g. the particle size, internal structures, and possibly particle density. A new method using atomic force microscopy (AFM) for the assessment of the effective particle density of individual spray-dried particles was demonstrated. In the second part, two different formulation concepts for encapsulation of protein during spray drying were developed. Both systems used non-ionic polymers for competitive adsorption and displacement of protein from the air/water interface during spray drying. The aqueous two-phase system (ATPS) of polyvinyl alcohol (PVA) and dextran, and the surface-active polymers, hydroxypropyl methylcellulose (HPMC) and triblock co-polymer (poloxamer 188) used for in situ coating, proved efficient in encapsulation of a model protein, bovine serum albumin (BSA). Inclusion of polymeric materials in a carbohydrate matrix also influenced several particle properties, such as the particle shape and the surface morphology, and was caused by changes in the chemical composition of the particle surface and possibly the surface rheology. In addition, powder performance of pharmaceutical relevance, such as dissolution and flowability, were affected.

Keywords: Spray drying, Particle formation, Density, Protein formulation, Encapsulation, Coating, Competitive adsorption, Polymer, ESCA, AFM, FTIR

Jessica Elversson, Department of Pharmacy, Box 580, Uppsala University, SE-75123 Uppsala, Sweden

ISSN l651-6192
ISBN 91-554-6322-3
urn:nbn:se:uu:diva-5904 (http://urn.kb.se/resolve?urn=urn:nbn:se:uu:diva-5904)

Till Mormor och Morfar

”Utan tvivel är man inte klok”
Tage Danielsson, 1928-1985

List of papers

This thesis is based on the following appended papers, which will be referred to by their Roman numeral, in the text:

I. Elversson J., Millqvist-Fureby A., Alderborn, G. and Elofsson U., 2003. Droplet and particle size relationship and shell thickness of inhalable particles during spray drying. J. Pharm. Sci. 92(4), 900-910.

II. Elversson J. and Millqvist-Fureby A. 2005. Particle size and density in spray drying–Effects of carbohydrate properties. J. Pharm. Sci. 94(9), 2049-2060.

III. Elversson, J., Andersson K.M. and Millqvist-Fureby A. A novel Atomic Force Microscopy approach for assessment of particle density applied to single spray-dried carbohydrate particles. Submitted to Eur. J. Pharm. Sci.

IV. Elversson J. and Millqvist-Fureby A., 2005. Aqueous two-phase systems as a formulation concept for spray-dried protein. Int. J. Pharm. 294 (1-2) 73-87.

V. Elversson J. and Millqvist-Fureby A., 2005. *In situ* coating–a novel approach for particle formation and encapsulation during spray drying. In manuscript.

My contribution

I am the sole contributor to the experimental work in all papers, except for Paper III were Karin M. Andersson carried out the AFM measurements and Paper IV where Tia Estey assisted with SEC-HPLC. Further, Nina Andersson performed the TEM analysis in Paper I; Andreas Sonesson contributed with the CLSM in Paper I and V; and Annika Dahlman performed the ESCA analysis in Paper IV and V. The BET-analysis in Paper II was performed at the Dept. of Chemical Engineering, Lund. I am the major contributor to the writing of the papers.

Other publications

Mollmann, S.H., Bukrinsky, J.T., Elofsson, U., Elversson, J., Frokjaer, S., Thalberg, K., Millqvist-Fureby, A. The stability of insulin in solid formulations containing melezitose and starch. Effects of processing and excipients. Manuscript to be submitted to Drug Dev. and Ind. Pharm.

YKI
YTKEMISKA INSTITUTET
Institute for Surface Chemistry

Contents

Abbreviations and symbols

A, B	Constants in equation 2
A_G	Orifice diameter of nozzle
AFM	Atomic force microscopy
ATPS	Aqueous two phase system
BET	Brunauer-Emmet-Teller
BSA	Bovine serum albumine
C_{bottom}	Concentration in bottom phase
C_{crit}	Critical concentration
CD	Circular dichroism
CLSM	Confocal laser scanning microscopy
CMC	Carboxymethylcellulose
COPD	Chronical obstructive lung disease
C_{top}	Concentration in top phase
C_{wb}	Concetration at wet bulb temperature
d	Particle diameter
d_a	Aerodynamic particle diameter
D	Droplet diameter; Diffusion coefficient
DSC	Differential scanning calorimetry
DST	Dynamic surface tension
DTGS	Deuterated triglycine sulphate
E_k	Kinetic energy
ESCA	Electron spectroscopy for chemical analysis
FTIR	Fourier transform infrared spectroscopy
g	Gravitational constant
hv	Specific energy of X-ray
HPMC	Hydroxypropyl methylcellulose
I	Intensity
k	Spring constant
K	Partition coefficient
m_{eff}	Effective mass
M	Mass
M_R	Air/liquid mass ratio
M_w	Molecular weight
MCT	Mercury cadmium telluride
P	Polymer
ΔP	Difference in pressure

PEG	Polyethylene glycol
PVA	Polyvinyl alcohol
PVP	Polyvinyl pyrrolidone
RH	Relative humidity
S_{wb}	Solubility at wet bulb temperature
SEC-HPLC	Size exclusion chromatography and high performance liquid chromatography
SEM	Scanning electron microscopy
STL	Tie-line slope
T_c	Crystallization temperature
T_g	Glass transition temperature
T_m	Melting temperature
$T_{storage}$	Storage temperature
T_{wb}	Wet bulb temperature
TEM	Transmission electron microscopy
UV/Vis	Ultra violet light/ visual light
V	Volume
V_{bottom}	Volume of bottom phase
V_{top}	Volume of top phase
VMD	Volume median diameter
z	Distance to surface; distance to reference point
% RH	Percentage relative humidity
% w/w	Percent by weight
α, β	Exponents in equation 2
γ	Relative coverage; Surface tension
ε	Porosity
η_l	Liquid viscosity
λ	Wavelength; Inelastic mean free path of photon
ν_0	Fundamental resonant frequency
ν_l	Loaded resonant frequency
ν_{rel}	Relative velocity air/liquid
π	Constant≈3.1416
ρ	Particle density
ρ_0	Unit density
ρ_a	Air density
ρ_{app}	Apparent particle density
ρ_{eff}	Effective particle density
ρ_l	Liquid density
ρ_t	True density
θ	Angle of emission
Φ	Correction for spectrometer work function
σ	Surface tension

Introduction

Pulmonary drug delivery

The respiratory tract is established as an attractive route for drug delivery. Small molecules such as β^2-agonists *e.g.* terbutaline (Bricanyl®), salbutamol (Ventoline®), salmeterol (Serevent®) and formetorol (Oxis®), and glucocorticoids, *e.g.* budesonide (Pulmicort®) and fluticasone (Flutide®), for local administration in the lungs, are all part of successful treatment of respiratory disease, such as astma, rhinitis, and chronic obstructive pulmonary disease (COPD). However, recent progress within biotechnology has generated a group of novel peptide and protein drugs to which administration to the respiratory tract, to obtain systemic delivery[1], seems advantageous compared to *e.g.* parenteral or gastrointestinal administration (tablets, capsules etc.). For example, the low metabolic activity in the lungs allows systemic delivery without liver passage[2]. Hence, the lungs is an attractive environment for biomolecules, which are highly susceptible to enzymatic degradation in the gastrointestinal tract (ventricle and guts) as well as hepatic degradation (first pass metabolism). In addition, the pulmonary route provides a large well-perfused surface area (~100 m^2) that allows for a higher absorption rate compared to the gastrointestinal tract. Moreover, the fragility of proteins, resulting in low chemical and/or physical stability in liquid formulation is a rationale for dried protein formulations. However, the respiratory system in itself restricts the entrance of particulate matter by various means: *e.g.* geometry of the airways and clearance mechanisms of the lungs. Consequently, inhalation particles have to be aerodynamically optimized to reach absorption sites in the alveolar epithelium.[3-5]

Conventional aerodynamic optimization means reduction of the particle size to less than 5 μm. Such particles are able to deposit in the alveolar tract but methods for size reduction, such as jet-milling can affect labile drugs and introduce changes in the physical properties of the particles[6], *e.g.* crystalline materials become amorphous. To overcome the detrimental effects of milling, spray drying can be an alternative, since particles in the appropriate size range can be produced directly.

An attractive strategy, in preparation of inhalation particles, is to manipulate both size and density of inhalation particles.[5] Stokes first law describes

the aerodynamic diameter (d_a) of a particle flowing in air with a physical particle size (d_p) and a particle density (ρ_p), where ρ_0 is unit density, 1 g/cm^3 (Eq 1). Particles larger than 5 μm are still able to penetrate into the alveolar region provided that the density of the particles is reduced to obtain a mean aerodynamic diameter of 1-3 μm, which corresponds to a density of <0.4 g/cm^3.[7]

$$d_a = d\sqrt{\frac{\rho}{\rho_0}} \qquad (1)$$

Pioneering work of Edwards et al.,[8] demonstrated that both aerosolization efficiency and delivered dose of inhalation powders could be increased when made of large porous particles. Firstly, an increased particle size results in a decreased tendency to aggregate[9], and in combination with a low mass, the aerodynamic behavior is retained or even improved.[8, 10] Secondly, phagocytic clearance can be diminished, by making particles larger since alveolar macrophages are unable to phagocyte units larger than about 5 μm.[11, 12] Large porous particles have been produced by several techniques, including spray drying.[7]

Theoretical aspects

Particle formation during spray drying

The spray drying process

Spray drying provides the possibility of formulating proteins and creating particles suitable for inhalation in one step. Formulations suitable for spray drying are solutions, suspensions and emulsions. In a typical spray dryer (Fig. 1a), the formulation is atomized into millions of small droplets, which are dried in a heated stream of gas into millions of small particles. Laboratory spray dryers, such as the widely used "Mini Büchi 190" (Büchi Labortechnik AG, Switzerland) use pneumatic nozzles, such as a two-fluid nozzle for atomization of the feed solution (Fig. 1b). The median droplet size is usually about 10 μm[13, 14] and particles suitable for inhalation can be formed. In contrast, production scale dryers are usually operated with rotating or pressurized nozzles, utilizing the centrifugal power or high pressure to disintegrate the feed liquid. In a co-current dryer the nozzle sprays in the same direction as the flow of the drying gas, which minimizes the thermal load on the droplets/ particles. Commonly used drying media are air or nitrogen. The spray-dried particles are separated from the drying gas by a cyclone or a bag filter (Fig. 1a).

Particle (surface) formation during spray drying

Droplet drying (solvent evaporation) starts instantaneously after atomization as the droplets meet the hot gas flowing through the dryer. Drying will proceed at a constant rate as long as the droplet surface is saturated (Fig. 2). During this short period (~10^{-4} s), the temperature at the droplet surface will be equal to the wet bulb temperature, T_{wb} (depending on the inlet and outlet temperatures). Simultaneously, dissolved material is transported through diffusion and convection to the surface of the droplet.[15] As was suggested in Paper I, a particle is established when the concentration at the surface reaches a certain level, the so-called critical concentration, C_{crit} (Paper I). C_{crit} will depend on the solubility of the material at T_{wb}, *i.e.* (S_{wb}) (Paper II).

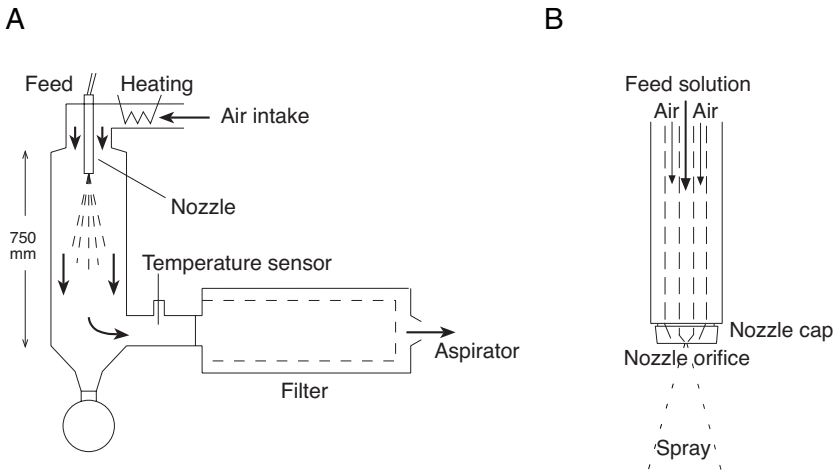

Figure 1. (A) Schematic picture of the spray-drier used in this thesis, equipped with a bag filter for particle separation. (B) Two-fluid nozzle.

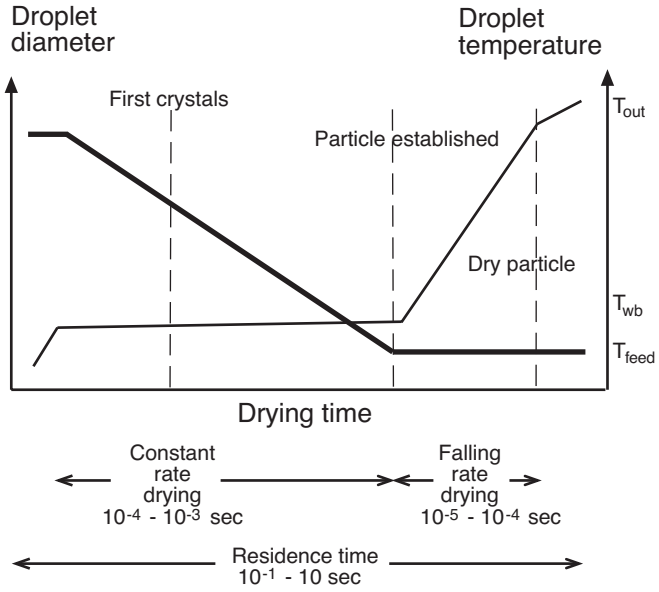

Figure 2. Schematic drying profiles showing the dynamics of size and temperature of the drying droplets of the spray dryer used in this thesis.

However, formulations containing surface-active components, such as surfactants or proteins separate during drying and the most surface-active component (under non-equilibrium conditions) is enriched on the surface of the drying droplet, irrespective of the solubility of the constituents. Several studies confirm that the composition of the droplet surface is preserved dur-

ing spray drying.[16-18] Consequently, when bovine serum albumin (BSA) or sodium caseinate is spray dried with lactose the protein is accumulated at the air-water interface[16] of the droplets and thus appears on the powder surface[16] (Fig. 3). In contrast, in a mixture of glycine and lactose neither of the components show any preferential accumulation and thus, the surface composition of the powder reflects the composition of the spray solution[16] (Fig. 3b). It is hence, important to control the surface competition during spray drying in order to create desired surface properties, *e.g.* wettability[19], dissolution (Paper V) or particle morphology (Paper IV-V).

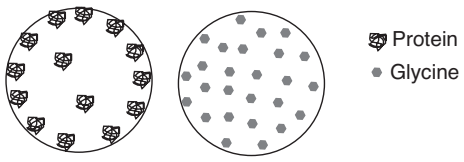

Figure 3. Schematic illustration of the surface composition of droplets during spray drying. (Left) Protein/lactose –enrichment of protein at the droplet surface, (right) glycine/lactose–no preferential adsorption. *Based on data from Fäldt and Bergenståhl, 1994.*

The relationship between droplet size and particle size during spray drying

Reasonably, the size of spray-dried particles will depend on the size of the initial droplet size. Although particle properties are highly affected by the air-liquid interface during atomization and drying the relationship between droplet and particle size during spray drying is a rarely investigated area, experimentally. However, as unit operations atomization, drying and separation are continuously investigated, within their particular field of interest.

Initial droplet size and droplet size distribution during spray drying can be altered by changing process parameters, such as the mass flow and velocity of gas and liquid through the nozzle[15, 20, 21] (Fig. 4a). Hence, changes of nozzle orifice diameter also affect the nozzle performance and the droplet size. Atomization with a pneumatic nozzle, such as the two-fluid nozzle follows the relation:[22, 23]

$$D = \frac{A}{\left(V_{rel}^2 \rho_a\right)^{\alpha}} + B\left(M_R\right)^{-\beta} \qquad (2)$$

where V_{rel} is the relative velocity between air and liquid in the nozzle, M_R is the air/liquid mass ratio (M_{air}/M_{liq}). The exponents α and β are functions of the nozzle design and A and B are constants related to both nozzle design and liquid properties.

In addition to process parameters, properties of the spray solution also play a major role in liquid disintegration (Fig. 4). Liquid viscosity, density and surface tension of the feed solution in a pneumatic nozzle correlate to droplet size according to the rather complex Kim-Marshall equation[23, 24]:

$$D = 5356\left(\frac{\sigma^{0.4}\eta_l^{0.32}}{\left(V_{rel}^2\rho_a\right)^{0.57} A_G{}^{0.36}\rho_l{}^{0.16}}\right) + \left(\left(\frac{\eta_l^2}{\rho_l\sigma}\right)^{0.17} \bullet \left(\frac{1}{V_{rel}^{0.54}}\right) \bullet \left(\frac{1}{M_R}\right)^m \bullet 3436\right) \quad (3)$$

where σ is the surface tension; η_l is the viscosity of the liquid; ρ_a, ρ_l is the density of air and liquid; and A_G is the orifice diameter of the nozzle.

For most pharmaceutical preparations liquid viscosity is probably the most important parameter to consider during spray drying and common polymers such as polyvinyl pyrrolidon (PVP) and hydroxypropyl methyl cellulose (HPMC) can change the viscosity substantially already at low concentrations.[25] Increasing viscosity results in larger droplets (Fig. 4) along with a reduced drying rate and diffusion of solutes.[26] In addition, some polymers are characterized by a non-linear relation between shear stress and shear strain rate. The atomization of non-Newtonian fluids can be difficult to predict and will apart from concentration also depend on the molecular weight of the polymer and the shear rate.[27, 28] Rigid polymers, such as xantan gum or carboxymethylcellulose (CMC) are extensionally strain thinning while flexible polymers are extensionally strain thickening and hence acts to "keep the fluid together". Consequently, spray drying of *i.e.* PVP, can result in elongated particles and tread spinning[29], which restrict the concentrations available during spray drying even further. According to Filková[30] non-Newtonian behavior should be considered for rotating and pressurized atomization whereas an apparent viscosity can be used for prediction of pneumatic nozzles.[20]

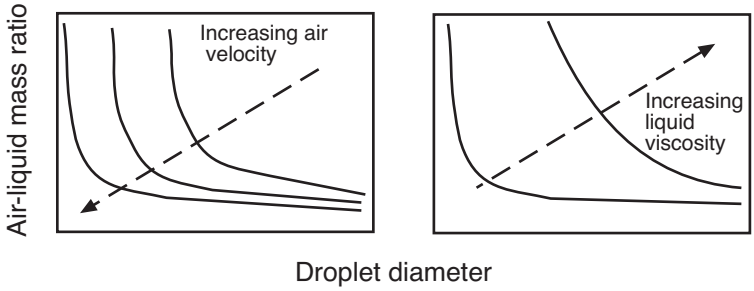

Figure 4. Typical performance of a two-fluid nozzle: droplet diameter as a function of air-liquid mass ration at changing (left) air velocity and (right) liquid viscosity.

Surface tension is the driving force behind formation of spherical droplets. Investigations on the relationship between surface tension and droplet

size during spraying contains contradicting information due to difficulties in defining the conditions (*i.e.* surface age) of relevance for the considered application.[31] Generally, the dynamic surface tension is a better predictor for droplet size than the equilibrium surface tension (Paper V).

As pointed out earlier, few studies discuss the effect of droplet size on particle size. For example, Dunbar et al.[32] report an influence of the operating pressure on the mass median aerodynamic diameter during spray drying of inhalable particles but unfortunately no investigation of the droplet size was reported, although the authors state that the reduced particle size was not correlated to the droplet size. Others have estimated the droplet size from particle size data by assuming non-porous particles[33, 34], which can result in an over-estimation of the droplet size if either porous or agglomerated particles are present during sizing.[15, 35] In addition, both the droplet size and the size distribution will change during drying[36] and drying kinetics for sprays are more complex[37, 38] and less well studied than drying of single droplets. Single drop drying includes both static and free-falling methods and for further information the reader is referred to a comprehensive review by Adhikari et al.[39] The results from investigations of static drying[40], where droplets are attached to a support or suspended in a gas stream (levitation), are difficult to apply to spray drying, due to large differences in time-scale, droplet size and flow conditions. Although more applicable to spray drying, the conditions in free-falling experiments can also be very different compared to spray drying.[41-44] Common experimental methods for the analysis of atomizer performance include laser diffraction[21, 45] (droplet size) and Phase-Doppler analysis (droplet size and speed).[46]

In conclusion, the relationship between droplet and particle size during spray drying deserves to be investigated further and Papers I and II discuss this in detail.

Adsorption of surface-active molecules during spray drying

Surface-active molecules such as small surfactants, proteins and polymers are common in liquid pharmaceutical formulations, where their purpose is to stabilize suspensions or emulsion from sedimentation, flocculation and coalescence; provide the formulation with suitable rheology properties and/ or a modified release profile. If such a formulation is designated for spray-drying the adsorption of the individual surface-active components at the air-water interface during atomization can become decisive for the particle properties[19], Further, if the active drug itself is a protein, competition for the air/water interface between different surface-active components in the formulation changes the extent of the surface adsorption and hence, the levels

of conformational changes in the protein molecules.[47, 48] Generally, protein (conformational) stability is better preserved when presence at the powder surface is reduced[49, 50] and hence surfactants and polymers such as poly(oxy ethylene sorbitan esters) (Polysorbate™)[18, 49-51], sodium dodecyl sulphate[52], and poly(ethylene oxide)-poly(propylene oxide)-poly(etylene oxide) (Poloxamer™)[50] have been used for protein stabilization during spray drying.

Transport to the air-water interface

The adsorption process for a protein or polymer at the air/water interface is usually divided into four main steps where transport from solution to a subregion close to the interface is the first stage. The other stages involve attachment to the surface, conformational changes at the surface and finally, displacement of segments initially adsorbed by other segments. Hence, molecules with a high affinity to the interface could exchange molecules with a low affinity[53], but the timescale of such exchange is likely to exceed the droplet lifetime.

The lifetime of droplets during spray drying is about 0.1-1 ms (Paper I-II), before the particle starts to solidify and the mass transport is restricted. Mass transport by diffusion and convection are the rate-limiting steps for adsorption, during spray drying.[17, 54] Consequently, amphiphilic molecules with a fast adsorption kinetics is in a superior position to more slowly adsorbing components, even if the latter can provide a lower equilibrium surface tension. Hence, dynamic surface tension rather than equilibrium surface tension should be used for prediction of accumulation and distribution of surface-active molecules during spray drying.

The quantity of protein or polymer that adsorb to the air/water interface is obtained by adsorption isotherms. Theoretically, approximately 1-3 mg/m^2 of most proteins is needed to reach full coverage of a surface, but depending on the orientation of the protein at the surface higher concentrations can be obtained.[55] Landström et. al reported an apparent particle surface load of BSA, during spray drying, of approximately 1.1-1.3 mg/m^2.[17, 56] This is comparable to adsorption isotherms obtained for a BSA monolayer on hydrophobic solid surfaces, (1.4–1.6 mg/m^2), as measured with radiotracer[57] and ellipsometry[58], respectively.

At fresh surfaces, with a low surface concentration of protein, the protein may unfold extensively and spread to cover the entire surface. During spray drying, the protein film changes from expanded to compressed, upon drying. A flexible protein can, particularly at low surface coverage rearrange and expose additional non-polar regions, leading to an increased binding strength to the surface.[48] Consequently, protein flexibility dictates the number of protein molecules that can adsorb to a surface and their spreading rate.[48] Approximately 50% surface coverage of protein monolayer is reached before any substantial decrease in surface tension is observed (induction phase).[59]

Thus, full surface coverage may be obtained (in the extended state), although, surface tension has not reached equilibrium.

Protein stabilization during spray drying

Formulation of protein pharmaceuticals is challenged by the low physical and chemical stability of proteins.[60, 61] Many processing steps, including spray drying, can cause conformational changes and initiate aggregation.[62] In its native state (active) proteins are folded into compact structures to minimize the thermodynamically unfavorable interaction between water and non-polar regions of the protein. The folded state will depend on the type of secondary structures (α-helix, β-sheet and β–turns) present in the protein. Denaturation or unfolding (inactivation) enables new combinations of ionic, hydrophobic and hydrogen interactions and especially globular proteins, such as lysozyme and albumin can form densely packed layers of strongly interacting protein molecules. Consequently, protein films can be extremely stable and hard to desorb (*e.g.* wash-off blood stains from clothing).

Improvement of the physical stability of protein drugs serves to: i) stabilize the native state; ii) prevent aggregation of unfolded structures; iii) prevent/ reduce interaction with interfaces; and iv) reduce shear forces. (For excellent review see Arakawa et. al[63] and Wang[62]). Various additives (*i.e.* sugars and amino acids) are found to reduce the damage and enhance the stability of proteins. In solution, the "preferential exclusion" of solutes in the immediate vicinity of proteins creates a thermodynamic situation where the native state is preferred before the unfolded state.[64, 65] Cryopreservation of proteins during freeze-drying follows the same mechanism as observed in solution. However, not all cryoprotectants are good stabilizers during dehydration. For example PEG is an excellent cryoprotectant but due to its hydrophobic character (increased affinity to unfolded protein) a poor lyoprotectant. During drying, the solute-induced stabilization is different from that in aqueous-frozen systems. Certain sugars are found to stabilize proteins during dehydration by a variety of mechanisms[66-70] (for details see below). Still, in many cases these additives are insufficient to completely stabilize proteins. During *e.g.* atomization, proteins in the formulation will accumulate at the air/liquid interface of individual spray droplets and possibly suffer from interfacial denaturation. Consequently, reducing the surface load of protein at the air/liquid interface during spraying by addition of surfactants or surface-active polymers can help preserve the activity of the bioactive protein.[18, 50-52]

Providing a suitable bulk

The glassy matrix

Excipients providing a glassy matrix demonstrate a much higher protectant effect compared to crystallizing solutes.[71, 72] For example, the residual activity of β-galactosidase initially after spray drying was approximately 109%, 81% and 42%, with addition of trehalose, mannitol and no stabilizer, respectively.[51] During accelerated storage the protectant effect was even more pronounced: 107%, 13% and 9%, residual activity, respectively[51]. The stabilizing effect has been explained by physical immobilization of the protein in the amorphous phase due to slow diffusion- and reaction rates.[67, 68]

Water replacement by sugars

Two sugars, sucrose and trehalose, appear especially efficient in freeze-drying and spray drying.[73, 74] Both sugars appear in organisms living under extremely cold or dry conditions and it has been shown that production of disaccharides is induced on desiccation, resulting in cell preservation until rehydration takes place. Although the mechanisms[66-70] behind sugar stabilization remains unclear an advancing number of reports indicate that solutes (sugar) providing hydrogen bonding to replace protein-solvent (water) interactions during dehydration are most successful.[75-77] Consequently, an excellent glass former but a poor protein protectant such as dextran, increase the thermal stability (increasing T_g) of the formulation but do not succeed in preserving the protein structure.[78-81] Hence, the stabilizing effect of sugars is concentration dependent. However, the mass ratio of protein-to-sugar appear to be of significant importance, not the bulk concentration.[82, 83] Consequently, loss of native conformation during dehydration can be observed both below and above the optimum concentration.[74] Based on differential scanning calorimetry (DSC) Imamura et. al found that the amount of BSA imbedded in one g of sucrose was 0.4 g.[84] Above that the excess BSA hydration is similar to BSA without sucrose.

From a spray-drying point of view, trehalose is very often preferred to sucrose, due to the higher glass transition temperature (115°C vs 74°C). Spray drying of trehalose can be performed at a higher inlet temperature[51], which result in a lower moisture content and hence a better storage stability.[51] In addition, the higher T_g of trehalose provides a larger difference between product storage temperature and T_g, which may extend the shelf life. A $T_{storage} \leq T_g$-30°C is generally aquired.[85, 86] However, an extension of the glassy state can be obtained by addition of a co-solute, such as dextran.[81]

Moreover, from a regulatory point of view, only non-reducing sugars are allowed in protein formulations. Reducing sugars (*i.e.* lactose) have the tendency to react with amino groups in proteins, forming dark brown aggregates, in a complex pathway. This reaction, known as the Maillard reaction is promoted by high temperatures.[87]

Reducing surface induced denaturation

As mentioned earlier, protein unfolding at the air/water interface can induce protein aggregation.[49, 50] Low-molecular surfactants, such as polysorbates[18, 50-52] adsorb much faster to the surface compared to *e.g.* trypsin and BSA, and a (partial) blocking of the surface is expected. More recently, improved survival rate was demonstrated from encapsulation of probiotic bacterium (*E. faecium*) in an aqueous two-phase system (ATPS)[29], containing PVP as the most surface enriched component. Similarly, the degree of encapsulation of BSA in a PVA/dextran ATPS (Paper IV) was controlled by the composition of the ATPS. Although PVA and BSA provided similar equilibrium surface tensions (approximately 50 mN/m[47, 88]) was the linear PVA molecules more efficiently adsorbed to the interface (Paper IV). In addition, flexible polymers such as block co-polymers (poloxamers) are spatially expanded[89] at the surface and hence very efficient surface blocking agents (Paper V).

Consequently, reducing the surface load of protein at the air/liquid interface during atomization by addition of surfactants or surface-active polymers is likely to prevent or delay the surface-induced denaturation of protein. This is particularly important for formulations with a low content of protein (active) where a large fraction of the total protein potentially will be distributed at the powder surface[90]. Hence, Paper IV and Paper V discuss new formulation strategies for protein pharmaceutics prepared by spray drying.

Characterization of spray-dried particles

The difficulties in characterizing spray-dried micro-particles, prepared by organic materials, such as carbohydrates, are due to both their small size and the material as such. Micro-particles are very cohesive, which causes problems during *e.g.* sizing (deaggregation), weighing and filling. Spray-dried carbohydrates are normally amorphous and hence hygroscopic but handling in a dry atmosphere tends to increase the cohesion and adhesion even more. In addition, the amorphous state limits the use of heat to remove moisture, which is necessary for accurate analysis of the particle surface area, particle density, porosity and chemical composition. Below follows some methods particularly suitable for characterization of density, surface composition, and structural integrity of proteins in spray-dried particles and which have been used in this thesis.

Atomic Force Microscopy (AFM)

From an inhalation perspective it is the effective particle density[91] that is relevant for the aerodynamic behavior of particles. The effective particle density includes both open and closed pores and thus, describes the (effec-

tive) volume excluded by the particle when flowing in air. Techniques available for measuring excluded volumes include liquid immersion, mercury porosimetry and gas pycnometry. However, the degree of pore penetration will depend on the dispersibility and wetting properties of the powder and of the pressure applied during analysis. The result will yield an apparent particle density[91], with a value more or less close to the density of interest. For example, solid particles (or particles without closed pores) obtain an apparent particle density close to the true density of the material as measured with helium pycnometry. However, for the spray-dried particles examined in this thesis none of the before mentioned methods could be used for obtaining the effective particle density. For example, the apparent particle density obtained by gas pycnometry (includes closed pores, but not open pores) can be three to four times as large as the density determined by mercury porosimetry.[92] And considering the small size of the particles reliable estimates of the average effective particle density is difficult to obtain by mercury intrusion.[93]

In an effort to assess the effective particle density of spray-dried carbohyrates, of a respirable size, an AFM was used as a balance for determination of particle mass.[94] The effective particle volume was accurately estimated from photographic pictures of the same particle. In the AFM, the mass of a single particle was obtained by measuring the shift in resonant frequency, when a spray-dried particle was placed at the end of a tipless AFM cantilever (Silicon MDT, Moscow, Russia), with a known spring constant.[95] In short, the method is based on the principles of an oscillating spring. An AFM cantilever is a beam type Hookean spring, the motion of which is described by the fundamental resonant frequency (ν_0) the effective mass of the cantilever (m_{eff}) and the spring constant (k):

$$v_0 = \frac{1}{2\pi}\sqrt{\frac{k}{m_{eff}}} \qquad (4)$$

Addition of a body (*e.g.* a spray-dried particle) with the mass, M at the end of the cantilever changes the loaded resonant frequency (ν_l)[94]:

$$v_l = \frac{1}{2\pi}\sqrt{\frac{k}{m_{eff} + M}} \qquad (5)$$

The AFM was used for measuring ν_0 and ν_l and by combing Eq. 4 and Eq. 5 the added mass, M, was determined.

$$M = k\frac{(1/v_l)^2 - (1/v_0)^2}{4\pi^2} \qquad (6)$$

The particle radius (r) used for assessment of the volume of the particle and estimation of the effective particle density (ρ_{eff}) was determined from photographic pictures.

$$\rho_{eff} = \frac{M}{\left(4\pi r^3/3\right)} \tag{7}$$

Electron Spectroscopy for Chemical Analysis (ESCA)

ESCA or X-ray photoelectron spectroscopy (XPS) provides the elemental composition of solid surfaces with a depth of analysis of 50-100 Å.[96] The instrument measures the kinetic energy (E_k) from photoelectrons emitted from atoms when the solid surface has been radiated with X-ray photons of a specific energy ($h\upsilon$). E_k is the excess energy when the binding energy of the element and orbital is lower than hν. The binding energy and hence the element of the electron is derived from:

$$E_k = h\nu - E_b - \Phi \tag{8}$$

where Φ is a correction factor for the spectrometer work function, which is characteristic for the spectrometer and the sample. The inelastic scattering of photoelectrons in solid matter result in an exponential decrease of the intensity (I) correlated to the distance from the surface (z).

$$I(z) = I_0 e^{-z/\lambda \sin\theta} \tag{9}$$

Hence, electrons far from the surface lose intensity and cannot be separated from the background. Consequently ESCA is an extremely surface specific technique.[96, 97]

Quantification of surface composition of pharmaceutical powders

The surface composition of the powder is estimated by analyzing the relative amounts of the different elements (*i.e.* carbon, oxygen, nitrogen) in the pure components (raw materials) and the powder samples. Each component in the powder is characterized by the specific ratio between the elements. By assuming that the elemental composition of the powder surface is a linear combination of the elemental compositions of the different components in the sample, the data of the elemental compositions of the pure components can be used to solve the matrix equation:

$$A\gamma = f \tag{10}$$

where A is the matrix containing the elemental compositions of the pure components; f is the vector containing the elemental composition of the sample surface and γ is the relative coverage of the different components. Over determined systems can be solved by applying the least-squares method for:

$$\gamma = (A^{\mathrm{T}}A)^{-1}A^{\mathrm{T}}f \qquad (11)$$

Dynamic surface tension (DST)

Conventional surface tension measuring methods, such as the Wilhelmy plate method and Du Nouy ring tensiometry, determine the static or equilibrium surface tension. Amphiphilic molecules, such as surfactants, consisting of hydrophilic (water-attracting) and hydrophobic (water-repellant) parts require much longer time than water and other liquids to achieve such a dynamic equilibrium. Processes such as foaming, spraying, and stirring rapidly form dynamic surfaces (area and shape of interface continuously changing) where air forms the hydrophobic surface. Hence, diffusion of the surface-active components is limiting in formation of surface tension.[53, 98]

Dynamic surface tension measuring methods, such as the pendant drop technique (Paper V) utilizes the opposing forces of gravity and surface tension acting on the droplet's shape (Fig. 5). Drops of test solution hang from a capillary (needle) and applying the Laplace equation of capillarity the surface tension can be derived from the radii of curvature of drops and the known force of gravity:

$$\Delta P = \gamma\left(1/R_1 + 1/R_2\right) \qquad (9)$$

where ΔP is the difference in pressure between the droplet and the surrounding air, γ is the surface tension and R_1 and R_2 are radii of curvature. Assuming gravity is the only external force acting on the droplet, the pressure difference can be expressed as:

$$\Delta P = \Delta P_0 + \Delta\rho g z \qquad (10)$$

where ΔP_0 is the pressure at a fixed point, $\Delta\rho$ the difference in density between the droplet and the air, g is the gravitational constant and z is the vertical distance from the reference point.

Programs for drop shape analysis take g, $\Delta\rho$ and the coordinates of several droplet points on the droplet's edge as input, and return surface tension, drop volume and surface area.

Other analysis techniques of dynamic surface tension include *e.g.* maximum bubble pressure (liquid/gas interface)[98, 99] and the sessile drop method (liquid/solid interface).

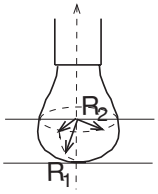

Figure 5. The pendant drop geometry.

Fourier Transform Infrared Spectrometry (FTIR)

The secondary structure of a protein is determined by the spatial orientation of the amide backbone, and the presence of hydrogen bonds. When the backbone angles have repeating values, the peptide forms regular secondary structures, such as the α-helix, β-sheet, or β-turn. Conformations that are not helices, sheets or turns are generally defined as unordered or random.

The IR spectrum of proteins arises from vibrational movements (stretching and bending) of the atoms in the peptide chain. In the Amide I region (1700–1600 cm^{-1}) bands correspond to the C=O stretch vibration, wheras the Amide II bands (1600–1500 cm^{-1}) origins from C-N stretching and N-H bending and the Amide III "the finger-print region" from a complex mixture of spatial displacements. Absorption in the Amide I region is best suited for assessment of the secondary structure of proteins[100] and different conformations (α-helix, β-sheet, or β-turn) absorbs at specific frequencies. Hence, helical proteins have a strong band between 1650–1655 cm^{-1} whereas proteins rich in β-sheet have a strong band between 1628–1635 cm^{-1} and a weaker band about 1685 cm^{-1}. The Fourier Transform is necessary for a sufficient signal-to-noice ratio of proteins in solutions.

Analysis of proteins with FTIR, in complex formulations, is related to certain precautions. Primarily, subtraction of the overlapping water signal in the Amide I region (1643.5 cm^{-1}) must be carefully undertaken.[100] The molar absorptivity of water is actually several magnitudes of order weaker than the strongest band of proteins but the high molar concentration is responsible for its very high net absorbance.[101] Therefore, liquid samples must be analyzed with a small path length, generally 10 μm or less. This unfortunately requires relatively high protein concentrations (>5 mg/ml) to achieve an adequate signal-to-noise ratio. In addition, residual vapor in the sample chamber must be carefully subtracted[100] from both liquid and solid spectra. Alternatively, formulations can be studied using D_2O (1555 cm^{-1}) but bands are shifted, and the continuous exchange of hydrogen in the sample to deuterium from the D_2O affects the position of various bands.[102, 103]

Circular Dichroism Spectroscopy (CD)

Circular dichroism appears when molecules absorb left and right handed polarized light to different extent. The chromofore in proteins is the amide bond which absorbs light below 250 nm. In the CD spectra the rigid α-helical structure forms a negative transition near 222 nm and second transition with a negative band near 208 nm and a positive band near 192 nm. The first transition is relatively independent of the length of the helix whereas the second transition decreases in intensity in short helices. The sheet conformation is more flexible than the helix and CD spectra of β-sheets display a negative band near 216 nm and a positive band near 195 nm, but the intensity and position of these bands is variable. β-turns display varying CD spectra. Among the eight types of turn structures, type I, II and III are most common in proteins and as a rule of thumb a negative band is located near 225 nm and a positive band between 200-205 nm.[104] CD and FTIR give complementary information regarding the secondary structure of proteins and a combination of the two techniques can determine the type of stabilization in a protein formulation.[105] For example, differences in the FTIR signal but not the CD spectra suggests that conformational changes in the protein involve hydrogen bonding since the CD spectra will depend on the bond angels in the peptide backbone whereas the FTIR spectra origins from changes in hydrogen bonds as well as bond angels.[105]

This thesis in perspective of current research

As concluded from the literature review previously presented, the potential of spray-drying within protein formulation lies in its ability to directly form particles with control of size, shape and density[7, 51], properties which are particularly important in the development of dry powders for inhalation. Not only is spray drying less time consuming as compared to freeze drying, it is also generally less energy demanding. In addition, certain pitfalls in protein formulation, such as solute concentration drying freezing[106], which can effect the pH and the ionic strength of the solution and thereby the protein stability, are avoided. Neither is any further processing, such as high energy milling, necessary, which otherwise can jeopardize the solid state stability.[6]

Despite the many advantages of spray drying, surprisingly few systematic studies on particle formation and how process and formulation parameters control the properties of the particles were found. It is for example relatively easy to change the size distribution in a spray by changes of the air-liquid mass flow ratio but the effect on the drying kinetics, shell formation, crust build-up and eventually particle size distribution remains to be shown. For example, the viscosity of the spray solution is most likely to cause an increase in the particle size, but in the case of non-Newtonian fluids, which include many pharmaceutical polymers, this behavior can be hard to predict. Also, excipients affecting the surface tension of the solution are likely influence the fluid break-up and hence droplet size during atomization.

Similarly, considerably less is known of protein stabilization during spray drying as compared to *e.g.* freeze drying. For example, concerns are raised about stresses during the spray drying process, caused by heating, pressure, shear[107], and interfacial expansion.[49, 50] However, the very large surface created in a spray indicate that the interfacial denaturation can be substantial during spray drying as compared to freeze-drying.[18, 49, 50] Consequently, reducing the surface load of protein at the air/liquid interface during atomization by addition of surfactants[18, 49-52] or non-ionic polymers[29, 107] can prevent or delay the surface-induced aggregation and deactivation of biomolecules.

In this light it became evident that the technical "knowledge" on understanding of spray drying needs to merge with the achievements within protein and peptide formulation during the last decades, and consequently two main subjects for this thesis were revealed. Firstly, understanding on how conditions during spray drying, and the type and concentration of the excipients interact and control the properties of the particles would lead to better

control and prediction of the spray drying process. In addition this improves the possibilities of designing particles suitable for inhalation, which can be produced from aqueous systems in a single-unit process. But in order to understand the mechanisms behind particle formation suitable methods for characterization of micro particles are needed. For example, to control the effective particle density, the effective particle density must be possible to measure. Today no such method is available for micro-sized non-solid carbohydrate-rich particles except indirectly, from aerosol deposition.

Secondly, the particular stress during atomization and drying of individual droplets, where proteins are exposed to the air/water interface may be more important during spray drying as compared to freeze-drying. Once again, knowledge of how the formulation affects the droplet size distribution during atomization becomes important. Process modifications or addition of surface active components may cause a decrease in the droplet size, which result in a larger total droplet surface area and a much more efficient transport of proteins to the air/water interface. Consequently, more interfacial interactions may result in more surface induced denaturation.[49] The increasing number of reports on protein stabilization during spray drying by surface exclusion point in this direction, and presently low molecular surfactants are added to protein formulations on a near routine basis. However, surfactants can also decrease the free energy of unfolding of some proteins, which may actually increase the risk of aggregation. For example, addition of polysorbate caused formation of large, insoluble aggregates of a hydrophobic lipase.[79] Consequently, new formulation concepts for effective encapsulation of protein in an aqueous matrix in combination with surface exclusion during spray drying are needed. Such formulation concepts would be especially valuable in low-dosage formulations where a substantial surface induced protein denaturation can be expected. In addition, surface modification of particles enables the possibility to design powder properties of pharmaceutical relevance, such as dissolution and flowability.

Aims of the thesis

With an overall objective to deepen the understanding of the formation of particulate systems for pulmonary administration of proteins, by spray drying, this thesis discuss two problems: How is the particle formation during spray drying affected by specific properties of the solute, in relation to particle size and particle density. Further, how can new formulation concepts be designed for concurrent encapsulation and prevention of proteins from surface induced denaturation during spray drying. The two areas were divided into the following specific aims:

- To investigate the influence of the droplet size during atomization and the solid content of the feed solution on the particle size and the particle density during spray drying of a common excipient, lactose. (Paper I).
- To study how the particle size and the particle density during spray drying of different carbohydrates (lactose, mannitol and sucrose/dextran 4:1) is related to properties of the solute, such as solubility and crystallization propensity (Paper II-III).
- To illustrate the origin of different internal structures in spray-dried carbohydrate particles by using a novel AFM approach for the assessment of the effective density of individual spray-dried carbohydrate particles. (Paper III)
- To evaluate aqueous two-phase systems (ATPS) as a formulation strategy to reduce or prevent surface induced conformational changes of protein during spray drying. (Paper IV)
- To influence specific particle properties and to reduce or prevent the surface induced conformational changes of protein during spray drying by *in situ* coating (Paper V).

Materials

Carbohydrates

Lactose

α-Lactose monohydrate (Merck Eurolab, Stockholm, Sweden) was used for the preparation of spray-dried particles in Papers I-III. Lactose is a naturally occurring disaccharide consisting of one galactose and one glucose unit (Fig. 6a). It is one of the most used pharmaceutical excipients but being a reducing sugar[87] not considered for protein formulations. Lactose easily becomes amorphous upon spray-drying and the glass transition temperature can vary between 120°C and 13°C depending on the amount of water incorporated.[108] In room temperature and with air at >44% RH lactose exsists above its T_g, as a super-cooled liquid and re-crystallization occur in matters of hours.[108] The water solubility of lactose is 20% w/w, at 25°C and 27.7% w/w at 45°C.[109] The apparent density of amorphous lactose is 1.48-1.51 g/cm^3 [110] and the true density of crystalline α-monohydrate is 1.53-1.55 g/cm^3.[25, 111] The refractive index of lactose was, n = 1.56.

Mannitol

D-mannitol dihydrate (Merck Eurolab, Sweden) was used for the preparation of spray-dried particles in Paper II-III. Mannitol is a sugar alcohol and unlike the other sugars used in this thesis a linear carbohydrate (Fig. 6b) Due to its very low glass transition temperature (13°C[112]) it has a strong propensity to crystallize and hence 89-100% of the mannitol crystallized during spray drying (Paper II). The water solubility of mannitol is 17% w/w[25] at 25°C and was determined to 29.3% w/w at 45°C (Paper II). The apparent density of crystalline mannitol is 1.51 g/cm^3.[25] The refractive index of mannitol was, n = 1.55.

Sucrose

Sucrose (VWR International, Sweden) was used for the preparation of spray-dried particles in Paper I-III. Sucrose is a disaccharide consisting of one glucose and one fructose unit (Fig. 6c). Neither of the rings is able to open (non-reducing) which renders sucrose suitable in protein formulations. The

water solubility of sucrose is high, 67% w/w at 25 °C[25, 109] and 71.1% w/w at 45°C[109]. Supersaturated solutions can remain stable for months without crystallizing (unpublished results). The glass transition temperature can vary between 57 and 13°C depending on the moisture content.[113] The true density of crystalline sucrose is 1.6 g/cm^3.[25] The apparent particle density can vary between 1.59–1.44 g/cm^3 depending on the amorphous content[6]. The refractive index of sucrose was, n = 1.50.

Trehalose

D (+)-Trehalose dihydrate (Fluka Chemie GmbH, Buchs, Germany) was used as filler and protein stabilizer in Paper IV and V. Trehalose is a non-reducing sugar consiting of two glucose residues (Fig. 6d) and one of the most commonly used carbohydrates for protein stabilization. The dihydrate exhibit two endotherms at approximately 100-120 °C assigned with dehydration and formation of the anhydrate, which melts at 211°C.[114] Amorphous trehalose has a glass transition temperature of 115-119°C [114, 115] and an apparent particle density of 1.54 g/cm^3 (Paper V).

Dextran

Dextran T40 (Amersham Pharmacia Biotech AB, Uppsala, Sweden, with a Mw of ~40 000 Da) was used in Paper II-III for the preparation of spray-dried particles. The water solubility dextran T40 is ~50% w/w, at 25 °C (according to the supplier). The apparent particle density of dextran (as received) was 0.96 g/cm^3 (Paper II).

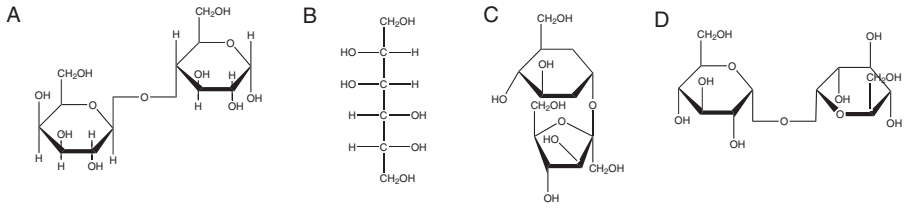

Figure 6. Structures of (A) lactose, (B) mannitol, (C) sucrose and (D) trehalose.

Polymers

PVA

Polyvinyl alcohol (Airvol 205, M_w~30 000 Da, Air Products Nederland BV, Utrecht, The Nederlands) was used in Paper IV for the preparation of the ATPS particles. PVA is produced from polyvinyl acetat (PVAc) and the

degree of hydrolysis was 88.26% (Fig. 7a). The glass transition temperature and the melting temperature of PVA was 49°C and 196°C, respectively (Paper IV). The surface activity of a PVA-solution at equilibrium is approximately 50 mN/m[88] and the diffusion coefficient, $D_{PVA} \approx 1.1 \times 10^{-9}$ m^2/s as measured by magnetic resonance imaging.[116]

Dextran

Dextran T70 (Amersham Pharmacia Biotech AB, Uppsala, Sweden, M_w~67 200 Da) was used in Paper IV for the preparation of ATPS particles. Dextran is a polysaccharide consisting of (1-6) linked α-D-glucose moieties, with a low degree (~5%) of branching (Fig. 7b). The glass transition temperature of dextran of this polymer lenght was 225°C (Paper IV).

HPMC

Hydroxypropyl methylcellulose (Aldrich, M_w~10 000 Da) was used in Paper V for the coating of protein particles. HPMC is a linear polymer composed of β4 linked glucose units. 29% and 8.8% of the C6 hydroxyl groups are substituted with metoxy- or hydroxypropyl groups, respectively (Fig. 7c). HPMC has a glass transition temperature around 170-180 °C, and browns and chars between 190-200°C.[25] The equilibrium surface tension is approximately 44 mN/m.[117]

Poloxamer

Poloxamer 188 (Synperonic™PE/F68, Uniqema, Gouda, The Netherlands; M_w~7680-9510 Da[25]), a poly(ethylene oxide)-poly(propylene oxide) triblock co-polymer with the following composition: PEO_{80}-PPO_{27}-PEO_{80}[25] was used in Paper V for coating of protein containing particles (Fig. d). The melting point is 52-55°C.[25] The equilibrium surface tension is approximately 40 mN/m[118] and the diffusion coefficient, $D=9.2\ 10^{-9}$ m^2/s.[119]

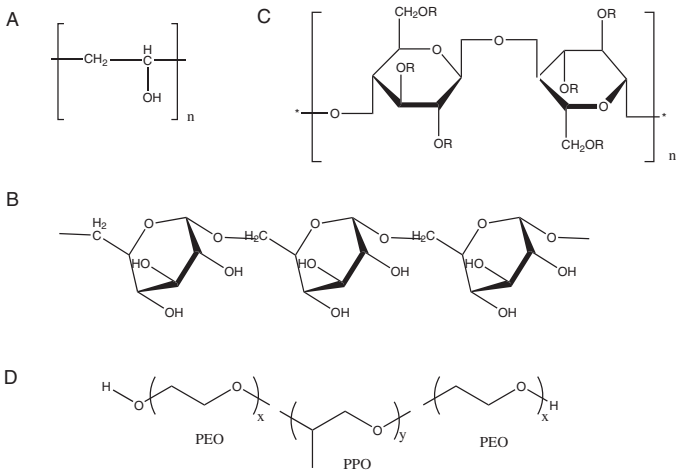

Figure 7. The structural elements of (A) PVA, (B) Dextran, (C) HPMC (R is H, CH_3 or $CH_2CH(OH)CH_2$) and (D) poloxamer.

Proteins

BSA

Bovine serum albumin (BSA), Cohn fraction V, >96% purity (Sigma Chemical Co., St Louis, MO, with a Mw of approximately 66 700 Da) was used in Paper IV and V. Serum albumin is a highly water-soluble globular non-glycosylated protein and the major plasma protein constituent (55% of the total plasma protein). Each molecule can carry seven fatty acid molecules, essential building blocks for membranes (lipids) and rich sources of energy. Albumins are easily purified and have been investigated as model proteins for chemical and physical studies for many years. BSA contains a single polypeptide chain with 583 amino acids, which include 35 Cys residues, 82 positively charged residues and 100 negatively charged residues.[120] The high total charge and many disulphide bonds contribute to its good solubility and stability.

BSA is characterized by high UV absorbance (λ=280 nm) due to 48 aromatic amino acids. The secondary structure has been estimated to contain about 55% α-helix and 10% β-turns.[120] The strong α-helix band at 1657 cm^{-1} dominates the FTIR spectrum of BSA. The circular dichroism of BSA in the far UV region shows minima at 209 nm and 222 nm and a strong maximum near 195 nm. The equilibrium surface activity of BSA in water is approximately 50 mN/m[47] and the diffusion coefficient, $D=6.7\ 10^{-11}\ m^2/s$.[121]

Buffer and dispersing agents

- Potassium bromide (KBr) (IR-grade, Sigma Chemical Co., St Louis, MO) was used for FTIR in Paper IV and V.

- Rapeseed oil (Karlshamns AB, Karlshamn, Sweden) was used in Paper I and II for dispersion of particles for laser diffraction analysis. The refractive index of rapeseed oil was, n =1.471.

- Fractionated cocunut oil, Miglyol 812N (Condea Chemie GmbH, Witten, Germany) was used in Paper I and II for dispersion of particles for laser diffraction analysis. The refractive index of cocunut oil was, n =1.448.

- Isopropanol (Solveco Chemicals, Täby, Sweden) was used in TEM analysis in Paper I.

- Cyclohexane (Sigma Aldrich) was used for preparation of samples for CLSM analysis in Paper III and V.

- Sodium phosphate buffer, prepared by dissolving NaH_2PO_4 and Na_2HPO_4 (pro analysi, Merck Eurolab, Sweden) in MilliQ water to 10 mM and pH 7.0, was used in paper IV and V.

- Water (MilliQ, Millipore Systems 18.2 MΩcm resistivity) was used for all preparations, in all experiments in Paper I-V. The refractive index of water was, n =1.00. Equilibrium surface tension was 72.2 mN/m (24°C).

- Fluoroscein isothiocyanate (FITC)-labeled BSA (Sigma Chemical Co.) was used in Paper V for CLSM.

Methods

Particle preparation

Carbohydrate solutions (Paper I-III)

Solutions of lactose, mannitol and a mixture of sucrose and dextran (4:1) were prepared at concentrations ranging from 1% w/w to saturated (*i.e*. 20% w/w, 15% w/w and 50% w/w). The solutions were allowed to stand for 1-5 hours prior to spray characterization and spray drying (Paper I-III).

ATPS solutions (Paper IV)

The ATPS solutions were prepared by mixing stock solutions (10% w/w) of PVA and dextran in different proportions. BSA solution (10% w/w) was added to the ATPS system to obtain a protein-to-polymer ratio of 5:95, on a weight basis. In formulations containing trehalose, an amount corresponding to 20% of the total polymer dry weight was dissolved in the BSA-ATPS solution, prior to spray drying (Paper IV). All solutions were prepared with a 10 mM Na-phosphate buffer at pH 7.0.

Coating solutions (Paper V)

Stock solutions (2% w/w) of HPMC were prepared by dispersing HPMC in cold buffer. When dissolved the HPMC solution was kept refridgerated for 24 hours to allow swelling and hydration of the polymer. Different proportions of the stock solution were added to solutions of BSA and trehalose to obtain a final concentration of 0.01, 0.1 and 1% w/w in solution. Similarly stock solution (2% w/w) of poloxamer in buffer was added to solutions of BSA and trehalose to obtain a final polymer concentration of 0.01, 0.1 and 1% w/w in solution. All solutions were prepared with a 10 mM sodium phosphate buffer at pH 7.0.

Spray drying

The spray dryer used in Paper I-V is a laboratory dryer built at the Institute for Surface Chemistry (Fig. 1a). The dryer operates in a co-current mode with a jacketed (25°C) two-fluid nozzle and the dimensions of the drying

column are 0.75 m in length and 0.15 m in diameter. The inlet temperature of the drying air was typically 200°C (Paper I-III) or 180°C (Paper IV-V) and the outlet temperature was kept at 90°C and 70°C, respectively. The flow rate of the drying air was 0.8 m^3/h. The orifice diameter of the nozzle was either 1.5 mm (Paper I-V) or 2 mm (Paper I-II) The flow of compressed air through the nozzle (*i.e* the atomization airflow) was varied between 20-32 L/min in Paper I while in Paper II-V it was kept at 28 L/min. Particles were recovered in a membrane filter (Gore-Tex Membrane, W.L. Gore & Associates Scandinavia AB, Mölndal, Sweden) (Paper I-III) or a cyclone (Paper IV-V).

Characterization of spray solutions

Dynamic surface tension (Paper V)

The dynamic surface tension of protein and polymer solutions in Paper V was determined with the pendant drop technique (First Ten Ångstroms, AccuSoft, version 1.961B) The surface tension at the air/solution interface was calculated from the size and shape of a droplet hanging from the tip of a syringe (BD 10 ml) with a blunt-end metal or teflon-coated needle (Hamilton Microlitre™ Syringes, Hamilton Bonaduz AG, Switzerland). All glassware as well as needles for the pendant drop analysis was washed in surfactant-free detergent (Deconex 20% NS, Borer Chemie, Switzerland) and thoroughly rinsed in de-ionized water and air dried before use. The surface tension of water as measured with the pendant drop was 72.2 mN/m (24°C).

Phase diagram and phase composition of ATPS (Paper IV)

The phase diagram of PVA-dextran in paper IV was determined by letting equal volumes of each polymer solution at each concentration (4-10% w/w) separate in graduated test tubes, at room temperature (23-25°C). The phase volume and the phase composition were analyzed after 21-24 hours of settling. Consequently, 1 ml of sample from each phase was withdrawn with a syringe and the PVA concentration in both top and bottom phases were determined at 280 nm (UV/Vis spectrometer Lambda 18, Perkin Elmer, Boston, MA). At this wavelength the absorbance of dextran was considered negligible and hence, the dextran content was calculated by mass balance from each withdrawn sample. The total solids content was obtained from drying the samples in a drying cabinet (UT6, Heraeus Instruments GmbH, Germany) at 105°C and >10 h.

BSA partitioning in ATPS (Paper IV)

Ten ml of BSA containing PVA-dextran solutions intended for spray drying were allowed to settle in test tubes as decribed previously. The concentration of PVA in each phase and BSA in the dextran-rich phase was recorded at 320 nm and 280 nm, respectively, with a corresponding ATPS without BSA used as a blank. The BSA in the PVA-rich phase was calculated from the total load of BSA, BSA in the dextran-rich phase and the phase volumes of settled systems. When, necessary, samples were diluted with buffer before absorbance measurements.

Solubility, refractive index and viscosity

The solubility of mannitol at 45°C in Paper II was determined by gravimetric analysis. Mannitol was added to water termostated at 45°C until the solution became saturated. The solution was filtered through a 0.2μm filter (Puradisc 25AS) and dried at 150°C (MA100, Sartorius AG, Germany) until the weight became stable.

The refractive indeces of spray solutions in Paper I-II were determined with a refractometer (Carl Zeiss SMT, Germany) at 20°C.

The kinematic viscosity (mm^2/s) of spray solutions in Paper I was measured with an Ubbelohde viscosimeter immersed in temperated water (25°C). A capillary with a constant k=0.004995 mm^2/s^2 was used for carbohydrate solutions and k=0.0524 mm^2/s^2 for polymer solutions.

Characterization of sprays

Droplet size distribution (Paper I)

The effect of nozzle orifice diameter, atomization airflow and feed concentration on the volumetric median droplet size (VMD) and size distribution of sprays were measured with laser diffraction (Malvern Mastersizer X, Malvern Instruments Ltd., Malvern UK) in Paper I (Fig. 8). In addition, the VMD was measured at different locations in the spray. In an effort to correct VMD for the loss of material to the walls of the drying tower of the spray drier, the high end of the cumulative size distribution was cut at the percentage corresponding to the powder yield during spray drying and hence, with a powder yield of 85% and droplet median diameter of 10 μm the corrected droplet median diameter became 8.5 μm (Paper I). Particle density and particle shell thickness was calculated from the corrected VMD.

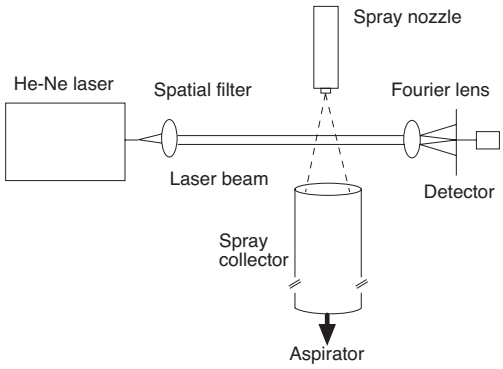

Figure 8. Setup for droplet analysis by laser diffraction.

Characterization of spray-dried particles

Morphology

The external and internal morphology of particles were inspected with various microscopy methods, such as SEM, TEM, CLSM and light microscopy

Scanning electron microscopy (Paper I-IV)

Forexternal and internal morphology imaging with SEM (ESEM XL30MP(W), FEI Company, Hillsboro, ON) particles were sprinkled onto Al-stubs covered by adhesive carbon tape and sputter coated (Sputter Coater SCD 50, Balzer Union AG, Lichtenstein) with Au/Pd of typically 640 Å thickness. The instrument used a HiVac SE detector and an acceleration volatage of typically 10-25 kV. SEM was used as a reference method to laser diffraction for particle sizing (Paper 1-II).

Transmission electron microscopy (Paper I)

For cross-section analysis with TEM (200FX, JEOL Inc., Akishima, Japan) particles were suspended in isopropanol and deposited onto carbon coated copper grids. The acceleration voltage was 200 kV.

Confocal laser scanning microscopy (Paper II and V)

For cross-section imaging with CLSM (LSM 510 Meta, Zeiss, Germany) the particles were dispersed in cyclohexane and deposited onto glass slides. Reflected light from an Ar laser (480 nm) was used to optically section the particles, using a pinhole diameter of 0.7 μm in from of the detector (Paper III). The 488 nm line in the Ar laser, with a LP 505 nm emission filter was used to image FITC-labeled BSA in particles with and without coating (Paper V).

Light microscopy (Paper II and III)

Particles intended for AFM analysis (Paper III) was imaged with a reflectance microscope (Optihot-100, Nikon, Japan) with a 50x objective

The fraction of low-density particles were also assessed by (Axioplan, Zeiss, Germany), equipped with a 40x/0.75 Ph2 and a 100x/1.30 oil objective (Paper II-III). To obtain a high contrast between solid matter and air particles were suspended in immersion oil and deposited into glass slides. The Axioplan microscope was also used for inspection of suspensions intended for laser diffraction analysis (Paper I-II).

Particle size distribution (Paper I-II)

Laser diffraction (Malvern MS2000, Malvern Instruments, UK) was used to determine the size distrubution (VMD) of spray-dried particles in Paper I-III. The instrument has a He-Ne laser and a Ar laser which enable detection between 0.02-600 μm. Before dispersing particles in liquid they were discharged by vacuum (<15 mbar) to facilitate dispersing. The dispersing agent was either rapeseed oil or coconut oil. Suspensions were ultrasonicated for 5 minutes before analysis in either a ultrasonic bath (Transonic T460/H) or with a 13 mm ultrasonic probe (Vibracell 750, Sonics & Materials Inc., CT).

Reported values are the volumetric median diameter (VMD) (Paper I-III), RANGE and SPAN values (Paper I). RANGE describes 80% of the particle volume while SPAN describes the variation around the median value according to Eqs. 11 and 12, where D(v, 0.1), D(v, 0.5) and D(v, 0.9) are the volumetric particle diameter at 10, 50 and 90% cumulative volume.

$$RANGE = D(v,0.9) - D(v,0.1) \tag{11}$$

$$SPAN = \frac{RANGE}{D(v,0.5)} \tag{12}$$

Apparent particle density (Paper II-IV)

The apparent particle density of unprocessed carbohydrates (Paper II and III) and spray-dried powders (Paper II-V) was evaluated by gas pycnometry (AccuPyc^{TM} 1330, Micromeritics, USA) using nitrogen and a 10 cm^3 or 1 cm^3 sample cell. Spray-dried lactose and mannitol in Paper II was also characterized with helium gas (>99.995% purity). The sample cell, filled to 2/3 with powder was purged with gas ten times before performing ten analysis runs. The pressure during purging and analysis was 134.4 kPa (19.5 psig) and the equilibrium rate was 34 Pa/min (0.005 psig/min). The sample weight was registered both before and after measurements.

Effective particle density (Paper III)

The density of single spray-dried carbohydrate particles was determined with AFM (MultiMode SPM, Nanoscope IIIA, Digital Instruments, USA). The spring constant of the rectangular cantilever was k=0.12 N/m and was calibrated with spheres of known mass.[95] Particles were attached to the cantilever by placing a minute amount of a sticky substance (ointment) at the apex of the cantilever and then transferring the particle to the cantilever using a micromanipulator and a glass fiber. It has been carefully controlled that the addition of the ointment does not influence the resonant frequency of the cantilever.[94, 95]. The radius and volume of the particle was determined from photographic images using a microscope (see Light microscopy).

Assessment of particle shell thickness (Paper I and III)

The median shell thickness of particles was calculated using the measurements of median droplet diameter, the median particle diameter and the concentration of the feed solution (Paper I). The shell thickness of individual particles was observed in photographic images taken with SEM (Paper I-II) and TEM (Paper I). Further the shell thickness of single hollow particles, classified as such by AFM, was estimated from light microscopy images (Paper III).

Surface area of powders (Paper III)

Spray-dried mannitol and lactose powders were subjected to gas adsorption by the multipoint Brunauer-Emmet-Teller (BET) method (ASAP2400, Micromeritics, USA) to obtain the specific surface area of the powder. The samples were degassed for 16–24 hours at 40 °C.

Chemical surface composition of powder (Paper IV and V)

The surface composition of spray-dried particles was analyzed with ESCA (AXIS HS photoelectron spectrometer, Kratos Analythical, UK). The instrument used a monochromatic AlKα X-ray light source. Powder was filled into DSC-crucibles, and placed under vacuum overnight. The pressure in the analysis chamber was ~10^{-8} torr. The circular analysis area was approximately 1 mm^2 and the depth of analysis was less than 100 Å.[19, 96] Analysis was performed in triplicates at different spots within a sample area of approximately 20 mm^2.

Thermal properties (Paper II, IV-V)

The physical state of solid samples was determined by DSC (822^e, STAR^e System, Mettler Toledo, USA). 40µl pinholed Al crucibles were used in all experiments. The heating rate was throughout 10°C/min and the nitrogen flow 40 ml/min. The degree of order (crystallinity) (Paper II) was calculated from the measured melting enthalpies (ΔH_{melt}) of spray-dried samples and of a completely crystalline sample. The powders were heated twice around the T_g to eliminate enthalpic relaxation. The T_g (midpoint) was determined in the second heating scan to allow comparison between samples. The theoretical T_g reported in Paper II for a spray-dried mixture of sucrose/dextran was calculated with the Gordon-Taylor equation[122], at 0% and 2% moisture content. Other transition temperatures, such as re-crystallization temperature, (T_c) and melting temperature, (T_m), reported in this thesis, are peak values unless otherwise stated. DSC was performed close upon spray drying to avoid any effects of storage.

Dissolution (Paper V)

In an effort to illustrate the dissolution behavior of in-situ coated particles 50 mg of sample was added to 1 ml of water (18°C) in a 1.5 ml vial. The sealed vials were continously rotated on a Heidolph Duomax 1030 rocking table (Rose Scientific, Edmonton, Canada) and the time for dissolution, as determined by visual inspection, was recorded.

Structural integrity of protein (Paper IV-V)

FTIR (Paper IV and V)

Transmission FTIR of both solid and liquid samples, reported in paper IV were performed at University of Colorado Health Sciences Centre, Denver, CO, using a Bomem HB 104 instrument (ABB Inc., Norwalk, CT) with a DTGS detector. Transmission FTIR and Attenuated Total Reflectance (ATR), reported in paper V, were performed on a Nicolet instrument (Nicolet Instrument Corp.) with a MCT detector.

For solid analysis spray-dried powder was dispersed in a KBr compact, at a protein to KBr ratio of 1:1000. For liquid analysis, spray-dried powders were rehydrated in water to a BSA concentration of 5 mg/ml, thereafter applied to a liquid cell with CaF_2 windows and a 6 µm spacer (transmission FTIR) or deposited onto a ZnSe crystal (ATR). The adsorption band of water (HOH bend vibration) is around 1644 cm^{-1} in transmission and 1636 cm^{-1} in ATR and hence, small spectral differences are observed between the two techniques upon analysis of aqueous protein solutions.[102, 103] The reproducibility between the methods has been estimated to 97% .[103]

CD (Paper V)

The secondary structure of BSA was assessed by a JASCO J715 spectropolarimeter at wavelengths between 180–275 nm. Spray-dried samples were rehydrated to 5 mg/ml of protein and diluted with buffer to a typical concentration of 0.12 mg/ml of protein for use with a 1 mm path length cuvette.

Size exclusion high performance liquid chromatography (SEC-HPLC) (Paper IV)

The amount of native protein and aggregates was quantified using a Tosoh Biosciences TSK-gel G2000SWXL column on a Hewlett-Packard (series II1090) HPLC (Palo Alto, CA) with UV detection at 280 nm. Spray-dried samples were rehydrated in water to 1 mg/ml and ultracentrifugated and 500 µl was applied to the column. The column was eluted with 10 mM Na-phosphate buffer (pH=7.0) at 0.6 ml/min. The amounts of native BSA and soluble aggregates were calculated from peaks eluting at 12.0 and 10.8 min, respectively. Results were expressed as peak percentage area of the total area.

Gel filtration (Paper V)

Gel filtration was conducted with a Superdex 200 26/60 column on a ÄKTA Explorer 100 (GE Healthcare, Uppsala, Sweden) with UV detection at 280 nm. Typically 5 ml of filtered sample (protein concentration 2 mg/ml) was loaded on the column at a flow rate of 2.5 ml/min. The mobile phase was a 10 mM sodium phosphate buffer with 0.15M NaCl at pH 7.0. The amounts of BSA monomer and soluble aggregates were calculated from peaks eluted after 193 and 165 ml, respectively. Results were reported as peak percentage area of the total peak area. The prescence of insoluble aggregates was determined by UV/Vis at 280 nm (Perkin Elmer Lambda 18 Spectrometer) in rehydrated samples before and after ultracentrifugation.

Results and discussion

Particle formation during spray drying

Droplet size

The results presented in paper I demonstrate how the median droplet size (VMD) during atomization can be increased from 6 μm to 20 μm by an increased orifice diameter of the spray nozzle and a reduced airflow through the nozzle (Fig. 9). Both measures decrease the relative motion of the atomization gas, thereby reducing the air-to-liquid feed ratio. The air velocity through the nozzle was decreased by approximately 56%, upon replacement of the 1.5 mm cap with a 2.0 mm cap. Thereby, the median droplet size was increased approximately 2.5 times. The effect from adjusting the airflow was smaller: twice as large droplets were obtained when decreasing the airflow from 32 to 21 L/min. For the larger nozzle a reduction of the airflow by 7 L/min generated 1.4 times larger droplets. The width of the droplet size distribution was increased as the droplet size was increased, for example RANGE increased from 10 μm to 30 μm by shifting from the small nozzle orifice diameter to the large orifice diameter. Further, droplets at the edges of the spray cone were approximately 30% larger than along the spray axis (Fig 10). Consequently the drying conditions experienced by individual droplets in the spray vary considerably. To obtain particles with a narrow droplet size distribution a reduction of the size distribution of the spray along the x and z direction (horizontal) might be beneficial.

Figure 9. Median droplet diameter as a function of atomization airflow and nozzle orifice diameter, 1.5 mm (open) and 2.0 mm (closed). Feed solutions: (○)water, (□)lactose 10% w/w, and (△) lactose 20% w/w.

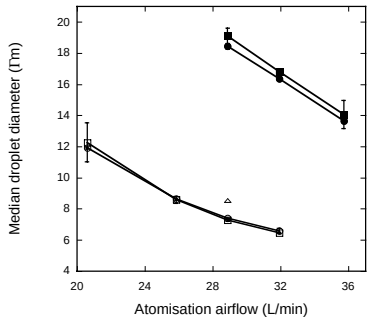

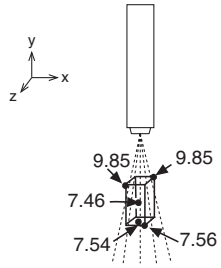

Figure 10. Median droplet diameter (μm) at different locations in the spray.

It was also found that carbohydrate solutions, such as lactose, without surface activity and only a moderate variation in viscosity (0.91–0.95 mPas) break up and disintegrate like water (0.89 mPas), at concentrations ranging from 1 to 20% w/w (Fig. 9). Mannitol solutions were assumed to behave similarly while sucrose solution with considerably higher viscosities (0.9-1.9 mPas) could be expected to increase the droplet size. However, analysis of sucrose solutions of <10% w/w showed profiles similar to water. More concentrated carbohydrate solutions were not possible to analyze due to contamination of the optics in the diffractometer. Thus, the droplet sizes reported was performed with water, to avoid distorted size distributions.

Regarding the effects on the droplet size from liquid viscosity it was difficult to perform such experiments due to the problems with lens contamination, as reported above, but unpublished data indicated an increase of the droplet size related to the measured kinetic viscosity (Table 1). The particularly large increase in the droplet size of the PVA solution might indicate a non-Newtonian behavior. Regarding the effects of liquid surface tension interestingly, no effects on the droplet size was observed for polysorbate solutions of varying concentration (0.005–0.5 mM). This might indicate that polysorbate has no effect on the surface tension at times relevant in atomization and particle formation. In contrast, inspection of *in situ* coated particles containing poloxamer (Paper V) by SEM showed a small reduction in the particle size, especially at a polymer concentration of 1% w/w of dry weight. Possibly the poloxamer lowers the surface tension more rapidly than *e.g.* polysorbate, and decrease the droplet size.

Particle size

As was expected, larger particles were obtained from sprays with a larger median droplet size. The correlation was linear (R>0.96) and independent of whether it was the larger nozzle or a lower airflow causing the effect on the droplet size (Fig. 11a).

Table 1. Median droplet diameter (VMD) as a function of viscosity and dynamic surface tension (pendant drop) of the spray solution. The nozzle orifice diameter was 1.5 mm and the airflow was 32 L/min. Mean values±SD (n=60).

Spray solution	Concentration (% w/w)	Polysorbate 80 (mM)	Surface tension (mN/m	Kinetic viscosity (mm/s)	VMD (μm)	RANGE
Water	–	–	~72	0.89	6.59±0.15	9.96
	–	–	~72	0.89	7.39±0.20[a]	10.5
Lactose	1	0.005	73.9[b]	0.91	6.96	10.4
	1	0.5	60.5[b]	0.92	6.83	12.4
	20	0.005	73.4[b]	0.95	7.07	11.5
	20	0.5	61.2[b]	0.95	6.84	10.5
Dextran	9.5	–		6.20	9.04[a]	
PVA	8	–		15.4	82.0[a]	
Ethanol	–	–	~23		5.03	33.7

[a]The nozzle airflow was 28 L/min.
[b]After 5 sec.

Paper I indicated that the relationship between the concentration of the feed solution during spray drying and the final particle size was nonlinear. Increasing the concentration of lactose in spray solutions from 5 to 20% w/w resulted in a moderate increase of the particle size (Fig. 11b). However, for very dilute solutions (1% w/w) significantly smaller particles were obtained (Fig. 11b) although the droplet size remained the same. The effect was observed with both laser diffraction (Fig 11b) and SEM (Fig 12). This relationship was later confirmed in Paper II for carbohydrates with different crystallization propensity and solubility, such as mannitol and sucrose/dextran (Fig. 13).

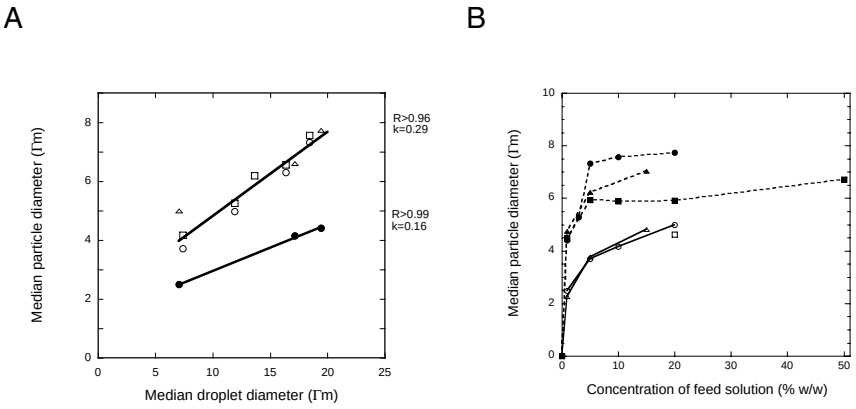

Figure 11. Median particle diameter as a function of (A) droplet size, and (B) the solids content of the feed solution. A: Solids content (●) 1% w/w; (○) 5% w/w; (□) 10% w/w (△) 20% w/w; B: spray-dried (●) lactose; (▲) mannitol and (■) sucrose/ dextran from two different droplet sizes (open=small, filled=large).

Hence, it might be assumed that the particle is established when the concentration at the surface of the drying droplet reaches a certain critical concentration (C_{crit}) (Paper I). At C_{crit} the diffusion of the solvent over the drying surface is lower than the heat transfer and the drying rate declines (falling-rate period). Paper I showed that C_{crit} could be calculated from the experimental data of droplet and particle size by assuming that the median diameter of the particles, as measured by laser diffraction, was equal to the droplet size at C_{crit}. However, the data of droplet size had to be corrected for the loss of material during drying. A simplified method was used to account for this, as described in the Experimental section.

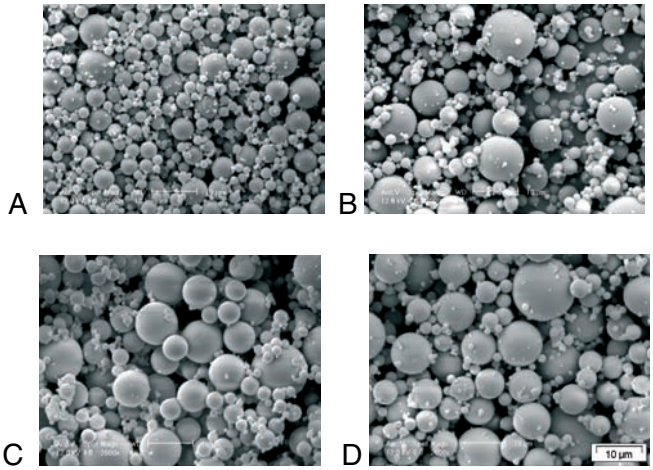

Figure 12. SEM micrographs illustrating the effect on particle size at different concentrations of the spray solution. (A) 1%w/w; (B) 5% w/w; (C) 10% w/w; and (D) 20% w/w of lactose.

Interestingly, the value of C_{crit} (24% w/w) was close to the solubility (28 % w/w[109]) of lactose at the estimated wet bulb temperature, (T_{wb}=45°C) during drying. In paper II the usefulness of the solubility at the T_{wb} (S_{wb}) in prediction of the median particle size during spray drying was confirmed by studies of mannitol and sucrose/dextran. S_{wb} was used for modeling the relationship between the particle size and the feed concentration of the respective carbohydrate solution (Fig. 13). Hence, the lower S_{wb} of sucrose/dextran resulted in smaller particles during spray drying. Consequently, the relationship between the particle size and the S_{wb} during spray drying appeared to be similar in solutes with different crystallization propensity. Satisfying correlations between yield compensated particle sizes and predicted particle sizes were obtained, with exception of mannitol produced from large droplets, where the particles were considerably smaller than predicted from the model (Fig. 13b). This may be due to that mannitol crystallize very fast, and considering the longer lifetime of the larger droplets (estimated to 0.8 ms for a 7 µm droplet and 56 ms for a 19 µm droplet), crystallization can occur to a

higher extent than for the smaller droplets. Thus C_{wb} will be higher (include dissolved and crystallized mannitol), allowing droplets to shrink to a smaller diameter before solidification. Further, the longer lifetime can explain the smaller particles obtained from the highest concentration of sucrose/dextran solution. Sucrose may form supersaturated solutions with a high stability, and thus droplets may shrink to give a concentration in the average droplet above S_{wb} before solidification occurs (Fig. 13c).

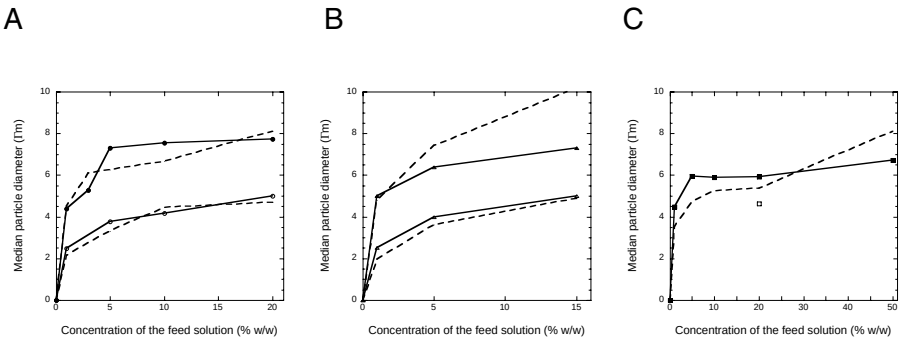

Figure 13. Median particle diameter as a function of the solids content of the feed solution. (A) lactose, (B) mannitol and (C) sucrose/dextran. Experimental data (solid line), predicted from S_{wb} at T_{wb} (dashed line), nozzle orifice diameter, 1.5 mm (open) and 2.0 mm (closed).

Also worth mentioning is that dismounting the nozzle cap of a two-fluid nozzle, *e.g.* during cleaning can cause small changes in the particles size. When the nozzle cap is re-tightened the adverse pressure in the nozzle can change and affect the droplet size. The variation in particle size caused by changing the cap was estimated ±0.14 μm. The typical standard deviation (SD) of the median particle size for a single sample was <0.02μm (n=10).

Particle density

Generally, spray drying results in non-solid particles. In accordance to our reasoning on C_{crit} and S_{wb} others report on the formation of smooth, flexible low-porosity skin on the droplet surface at a certain stage[123] for skin-forming materials.[40] If all particles from spray drying were solid (*i.e.* no vacuoles), then particles obtained from the droplet sizes reported in Paper I would have been considerably smaller. For example, a 10% w/w lactose solution with a droplet size of 6.4 μm resulted in particles with a particle size of 4.2 μm, while a solid particle would have been 2.6 μm in diameter. In addition, provided that the droplet size remained unchanged, increasingly larger particles would be produced from solutions with an increasing concentration. However, the considerably larger particles observed from the spray drying experiments presented in this thesis (Fig. 12b) can be explained by the forma-

tion of non-solid particles. Consequently, a higher concentration of the spray solution would result in more dense particles, with a thicker shell. Figure 14 illustrates the shell in amorphous lactose and sucrose/dextran particles as well as the internal structure of a crystalline mannitol particle. From this follows that the density of spray dried particles appear to be low and hence spray drying results in particles with a suitable aerodynamic diameter (Eq 1). Table 2 summarizes the effective particle density calculated from droplet-to-particle measurements and the apparent particle density as measured by gas pycnometry. The discrepancy between the effective particle density and the apparent particles density obtained by gas pycnometry may suggest that the particles were highly permeable to nitrogen, which was used as intrusion medium. The uncertainity in using gas pycnometry for analysis of spray-dried porous particles has been reported.[92] Somewhat similar to what was reported in Paper IV and V, where a decrease in the apparent particle density correlated with a higher coverage of polymer at the surface of the particles, a lower apparent density, as measured by gas pycnometry, was correlated to high solid contents (Table 2). The contention that gas permeability is of importance for the apparent density of non-solid particles was further corroborated by BET data for lactose and mannitol powders (Paper II).

Table 2. Effective particle density calculated from droplet-to-particle measurements and apparent particle density measured by gas pycnometry.

Carbohydrate (True density)	Lactose (1.55 g/cm^3)[a]		Mannitol (1.51 g/cm^3)[a]		Sucrose/ dextran (1.59 g/cm^3)[a, b]	
Particle density (g/cm^3)	Effective	Apparent	Effective	Apparent	Effective	Apparent
Feed conc. (% w/w)	Nozzle orifice diameter (1.5 mm)					
1	0.20	1.55	0.16	1.51	–[c]	1.55
5	0.21	1.54	0.24	1.50	–[c]	1.53
10	0.38	1.53	–	–	–	–
15	–	–	0.30	1.49	–	–
20	0.25	1.50	–	–	0.31	1.52
Feed conc. (% w/w)	Nozzle orifice diameter (2.0 mm)					
1	0.34	1.55	0.28	1.49	0.47	1.54
3	0.49	1.53	-	1.48	–	–
5	0.19	1.54	0.51	–	0.48	1.55
10	0.21	1.49	-	1.47	0.68	1.54
15	–	–	0.88	–	–	–
20	0.36	1.45	–	–	0.72	1.52
50	–	–	–	–	1.67	1.33

[a]By gas pycnometry (unprocessed powders)
[b]Sucrose
[c]Data on particle size not available.

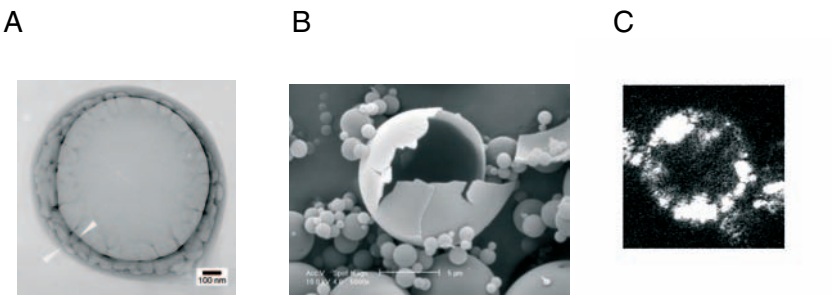

Figure 14. TEM, SEM and CLSM micrographs of the internal structure of spray dried carbohydrate particles: (A) lactose, (B) sucrose/dextran, and (C) mannitol.

Single-particle density

Since the apparent particle density obtained by gas pycnometry was poorly correlated to the theoretical densities as calculated from the droplet-to-particle measurements, particles were analyzed with a newly developed method using AFM[94] (Paper III). Generally, spray-dried carbohydrate particles analyzed with AFM had surprisingly high effective particle densities, ranging from 0.78 g/cm^3 to 1.47 g/cm^3 (Fig. 15), considering the relation between the median droplet size and the median particle size, suggesting and average density of 0.4 g/cm^3 (Table 2). There appeared to be no correlation between the effective particle density and the particle size but results from each sample concentrated in two separate groups for lactose (Fig. 15a) and sucrose/dextran (Fig. 15b) while mannitol (Fig. 15a) only displayed one population. The separation in two populations was verified with microscopy, where particles could be classified as either “hollow” or “solid” depending on the appearance of the particle interior (Fig. 16). Paper I-II showed that lactose and sucrose/dextran were amorphous while mannitol was >89% crystalline. A hypothesis on the formation of different internal structures related to the crystallization propensity of the solute was suggested in Paper II. This was further supported by measurements of droplet-to-particle size, apparent particle density by gas pycnometry, and by cross-sections taken with various microscopy techniques (SEM, TEM, CLSM) illustrating differences in internal structures (Paper I-III). Hence, hollow spheres were associated with amorphous materials (such as lactose and sucrose/dextran), while carbohydrates which crystallized during drying (such as mannitol) formed low-density particles with a different internal structure (porous).

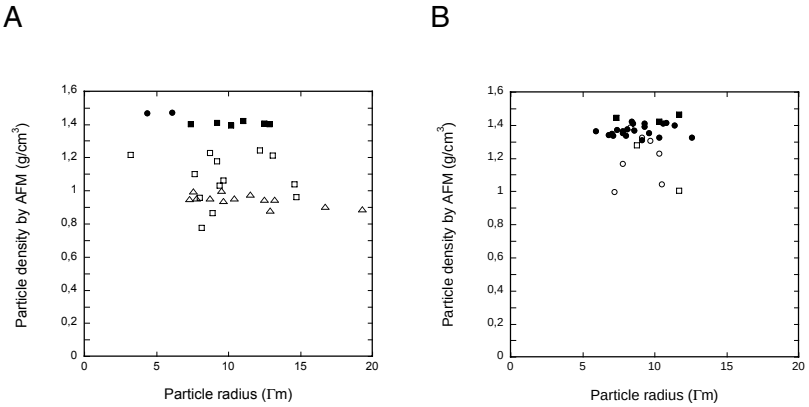

Figure 15. Effective particle density assessed with AFM: (A) lactose 5% w/w (●); lactose 20% w/w, solid (■) and hollow (□); mannitol 15% w/w (△); (B) sucrose/dextran 20% w/w, solid (●) and hollow (○); and sucrose/dextran 50% w/w, solid (■) and hollow (□).

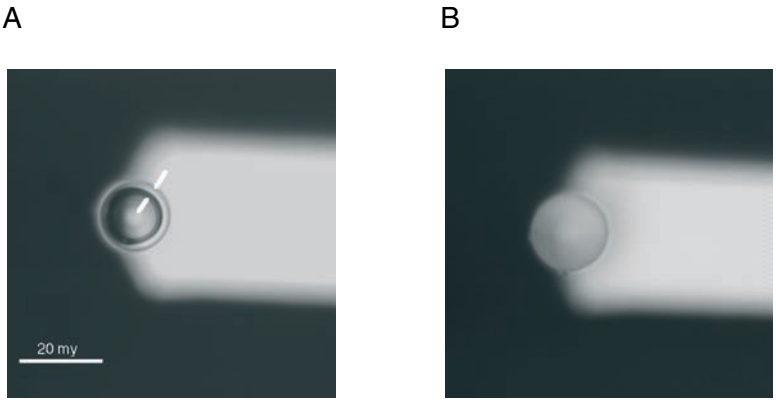

Figure 16. Photographic pictures illustrating a hollow particle (A) and a solid particle (B) attached to the rear end of an AFM cantilever. The thickness of the particle shell is illustrated with arrows.

Further, the variation in the effective particle density of hollow spheres was large as compared to the range of densities obtained for solid particles (Fig. 15). Although the particle density appeared independent of the particle size a positive linear relation was found between the shell thickness and the size of lactose and sucrose/dextran particles (Fig 17). Shell thickness of individual particles was estimated from the photographic pictures used for volume determination (Fig. 16). The calculated density of the particle shell corresponded fairly well with the true density of each carbohydrate (Table 2) and hence we believe that particles of amorphous carbohydrates, such as

lactose and sucrose/dextran actually are hollow, with a close to compact shell and that the shell can be observed by microscopy (Fig. 16a).

A limitation of the AFM method, in the context of spray-dried micro-sized powders, is that only particle larger than 10 μm can be measured. Further, this rather laborious technique also limits the number of particles that can be analyzed. Thus, a small and skewed selection of the particle population is investigated, but the results still point at that the particles indeed are porous to a large extent.

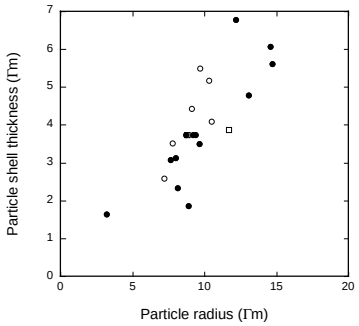

Figure 17. Shell thickness of particles as measured from photographic pictures: lactose 20% w/w (●), sucrose/dextran 20% w/w (○) and sucrose/dextran 50% w/w (□).

Protein stabilization during spray drying

Aqueous two-phase systems as a formulation concept

A different, and until now unexplored, approach for prevention of protein adsorption at surfaces and improvement of its stability in the dried state is encapsulation in an ATPS (Fig. 18).[124] In an ATPS, formed by two non-ionic polymers, phase separation occurs at very low concentrations.[125] and the origin of this polymer incompatibility is the small entropy of mixing of large polymer molecules combined with an enthalpic contribution favoring phase separation. During drying the phase separation may even proceed further as the polymer concentrations increases[126], although the extent of this may be limited in such a rapid process as spray drying. Due to the low interfacial tension (between 10^{-4} and 10^{-1} mN/m compared to 1–20 mN/m for conventional water-organic interfaces) between the polymer phases adsorption of protein at the liquid-liquid interface is less likely.[127] Further, the low interfacial tension implies that only a low level of energy is required to obtain and maintain an emulsion structure in the ATPS. The point of using an ATPS in protein formulation is summarized below:

- To prevent surface induced denaturation
- To provide an efficient encapsulation
- Offers a possibility to control release properties
- May improve long-term stability (observed for bacteria[29])
- Water as solvent in both phases

The ATPS described in Paper IV was successful in terms of protein encapsulation during spray drying, thus minimizing the exposure of proteins to the air-liquid interface of the drying droplets. As concluded in paper IV an ATPS must fulfil certain criteria and hence PVA and dextran was selected according to the following:

- PVA and dextran formed an ATPS at such concentrations that the viscosity of the solution was low enough to enable spray drying.
- Neither PVA (with this M_w and at the concentrations investigated here) nor dextran exhibited any appreciable extensional viscosity, which could impart the particle formation during spraying.
- The T_g of the respective polymers was high enough to allow particle preparation by spray drying.
- BSA preferentially partitioned to the dextran phase.

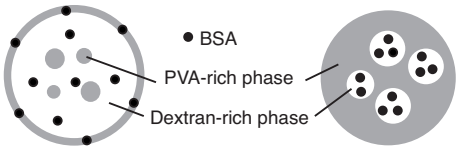

Figure 18. Schematic illustration of the BSA partioning in ATPS droplets before and after phase inversion, resulting in different surface compositions during spray drying.

Phase diagram of PVA-dextran

Figure 19 shows the phase diagram and phase compositions of the PVA-dextran ATPS, determined at 21–23°C. In a stirred system the continuous phase is the polymer phase with the largest phase volume. Phase inversion of the PVA-dextran system occurred at approximately equal phase volumes, in this case at a 1:1 PVA:dextran ratio.

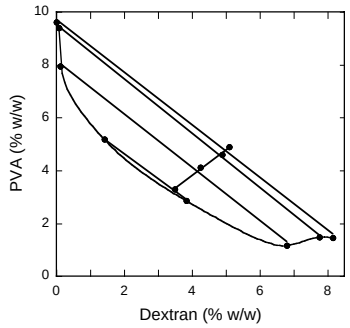

Figure 19. Phase diagram of PVA and dextran in 10mM phosphate buffer, pH=7.0 (STL=-1.006±0.035).

BSA partitioning in PVA-dextran

BSA strongly partitioned to the dextran-rich phase of the PVA-dextran ATPS (Table 3). In the case of equal concentrations of both polymers, 84% of the BSA was detected in the dextran-rich phase.

Table 3. Partitioning of BSA in PVA-dextran ATPSs, with varying polymer compositions. Mean±SD (n=2)

PVA content of total polymer (%)	V_{top}/V_{bottom}	K	Percentage BSA in bottom phase (%)
0	–	–	–
10	0.04±0.01	0.66±0.05	98±1.0
20	0.14±0.03	0.48±0.14	94±0.6
25	0.20±0.03	0.39±0.05	93±0.2
50	0.80±0.04	0.24±0.02	84±0.3
100	–	–	–

Powder surface composition and effects on particle properties

The content of the surface-active components, such as BSA and PVA in the ATPS strongly affected the surface composition of the spray-dried particles. In dextran 64% of the surface was found covered with BSA which is comparable with reported values in similar protein–carbohydrate systems[16, 17] (Fig. 19). The reason for the high surface load of protein is that the surface-active BSA adsorbs to the air-water interface during atomization. Upon addition of PVA, the surface coverage of BSA was substantially reduced and PVA was enriched at the surface. Complete surface coverage with PVA was achieved at 25% PVA content of total polymer (Fig. 20). BSA and PVA possess similar equilibrium surface activities (approximately 50 mN/m[47, 88]) but due to the higher diffusion coefficient of PVA ($D_{PVA}=1.1x10^{-9}$ m^2/s[116] compared to $D_{BSA}=6.7x10^{-11}$ m^2/s[121]), the polymer is kinetically favored and acts as an encapsulant, even when the PVA-rich phase is the dispersed phase. Addition

of trehalose did not change the surface composition of spray-dried ATPS particles (Fig. 20).

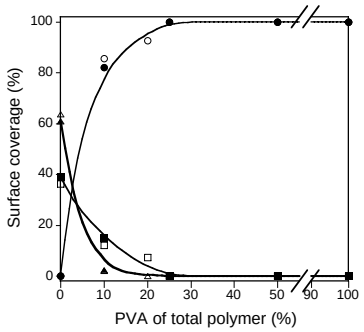

Figure 20. Surface composition estimated by ESCA, illustrating the surface coverage of (●) PVA, (■) dextran and (▲) BSA in ATPS powders with (filled) and without (open) trehalose.

The surface morphology of the spray-dried particles was also correlated to the surface composition; encapsulation of BSA with PVA changed the morphology from wrinkled raisin-like particles to smooth spheres, as the content of PVA increased from 0–100% of the total polymer (Fig. 21). Based on the findings in Paper V differences in the BSA[128, 129] and PVA[128] film rheology may be the cause of different surface morphology. Variations in the properties of the surface film could possibly also explain the differences in the apparent particle density observed by gas pycnometry. The apparent particle density decreased linearly from 1.4–0.4 g/cm^3 upon an increase of the PVA content from 0–100% of total polymer (Table 4). Film-forming polymers such as PVA are likely to form a dense ("gas-resistant") shell during spray drying. Upon higher concentrations of PVA the adsorbed polymer layer increases in density or thickness[130] and hence less nitrogen reaches the interior void, thereby increasing the apparent volume of the particle. Dextran is likely to be permeable to nitrogen, as observed for disaccharides (Paper II), and since the interior void is more or less reduced, the apparent particle density will be close to the true density of the materials.

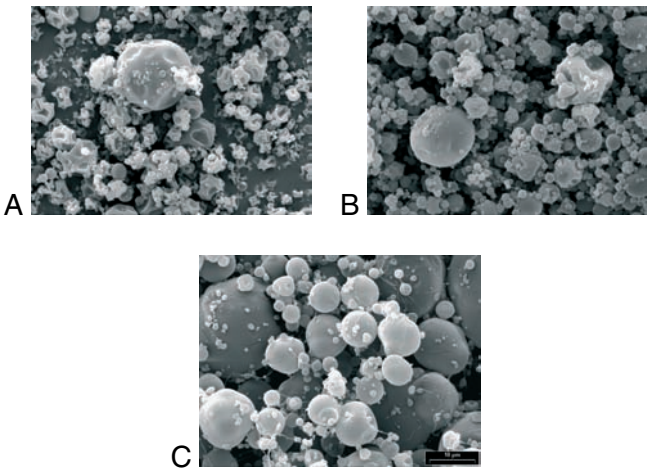

Figure 21. The morphology of spray-dried ATPS particles was affected by the surface coverage of PVA. (A) 0%, (B) 10% and (C) 100% PVA of total polymer. Bar lenght 10 μm.

Table 4. Apparent particle density, by gas pycnometry, of ATPS particles. Mean value, SD<0.005 (n=5–10)

PVA (% of total polymer)	PVA–dextran (5% BSA) (g/cm^3)	PVA–dextran–Trehalose (5% BSA) (g/cm^3)	PVA–dextran (10% BSA) (g/cm^3)	PVA–dextran–trehalose (10% BSA) (g/cm^3)
0	1.33	1.35	1.32	–
10	1.26	–	–	–
25	1.09	1.21	–	–
50	0.75	0.87	0.91	0.79
100	0.40	0.54	–	0.49

Structural effects on BSA

As expected, dextran alone failed to protect BSA during drying.[78-81] Only 57% of the helix structure of BSA was retained in dextran which is comparable to other studies on proteins co-dried with dextran[77] (Fig. 22). However, FTIR also demonstrated that considerable loss of native structure of BSA occurred during spray drying of ATPSs although the protein was embedded in a matrix, preventing it from interacting with the air/water interface during spray drying (Fig. 22). Band broadening, extensive loss of α-helix content and appearance of β-turn and β-sheet in dried samples correlated with the high amount of aggregates measured with SEC-HPLC in rehydrated samples (Paper IV). The observed changes of BSA integrity were correlated to the content of PVA. An unexpected interaction (hydrogen bonding) between PVA and the protein during spray drying was the likely cause of the PVA induced destabilization of BSA. Thus, the encapsulation of BSA in the ATPS cannot prevent the interactions between protein and PVA that distort

the protein structure. Possibly, PVA incured the unfolding in the solid state, that may have fostered the aggregation upon rehydration, although it can be assumed that the denaturation at the air-liquid interface is prevented through encapsulation.

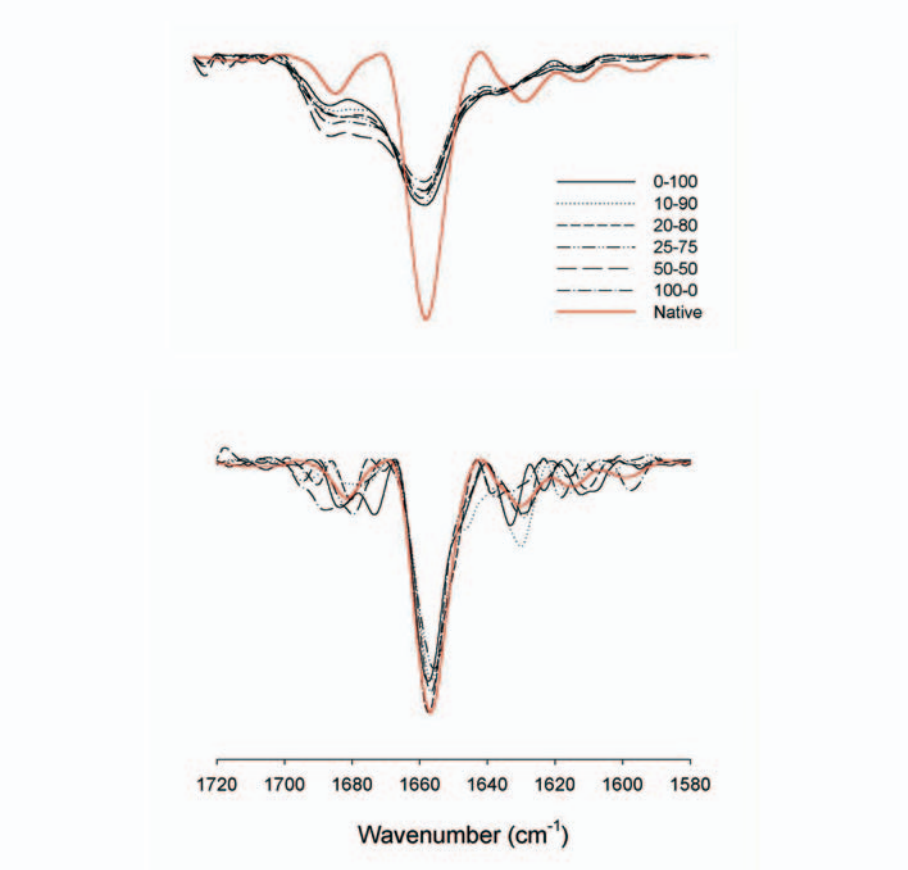

Figure 22. Second derivative amide I spectra of BSA spray-dried in ATPS with a varying composition of PVA–dextran (% of total polymer), before (upper) and after (lower) reconsitution of powders in water.

Effects of trehalose

Trehalose was added to the formulations as a filler and for its supposed protein stabilizing effect (protein:sugar mass ratio of 1:3.8) but the effect was limited, α-helix content was only slightly improved. However, trehalose reduced the structural variability in samples and interacted with dextran (true mixtures), which was observed as a narrowing of the helix band (Paper IV) and a lower glass transition temperature (Paper IV), respectively, and hence trehalose may benefit from a higher dosage. However, it is questionable if

the PVA–protein interaction can be overcome by addition of trehalose. The ATPS concept would most likely be more beneficial with a different choice of polymers, where no negative interaction occur.

In situ coating of protein particles

Paper V presents a novel method for *in situ* coating of protein-containing particles of a respirable size (Fig. 23). The aim of the coating was to influence the powder properties, and to reduce or prevent surface-induced conformational changes of the protein, during spray drying.

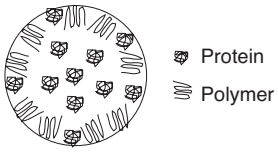

Figure 23. Schematic illustration of the surface composition of an *in situ* coated droplet during spray drying.

Dynamic surface tension determines the chemical surface composition

Due to the very short life-times of droplet surfaces during spray drying adsorption kinetics of surface-active components in the formulation become more important than equilibrium surface tension. Hence, molecules adsorbed at the surface in the moment of shell formation will remain there during drying. The dynamic surface tension of a formulation depend on the competitive adsorption of components at the air/water interface. Consequently measurements of the dynamic surface tension can help predict the component most likely to cover the surface of spray dried particles.[16, 54]

The surface tensions (at equilibrium) of HPMC and poloxamer is comparable, 44 mN/m[117] and ~40 mN/m[118, 131], respectively, but the poloxamer adsorps to the air/water interface much faster compared to the HPMC, during the time scale relevant in spray drying (Fig. 24) However, approaching equilibrium the dynamics of rearrangements and displacements of poloxamer[89] exceeds those of HPMC[132] (days vs hours).

Since the dynamic surface tension of the protein-polymer mixtures followed the kinetics of the pure polymer both coating polymers, HPMC and poloxamer 188 appeared efficient for coating and encapsulation of BSA (Fig. 24). This was confirmed by ESCA analysis of the chemical surface composition of spray-dried powders (Fig. 25). At a polymer concentration of 1% w/w of dry weight no protein or only low levels (1.7%) of protein were detected on the surface of spray-dried particles coated with HPMC and poloxamer, respectively. At polymer concentrations lower than 1% w/w increasing levels of BSA were detected at the particle surface and uncoated particles displayed a mixed surface of BSA and trehalose, containing ap-

proximately 57% BSA (Fig. 25). This level is lower compared to surface coverage of BSA spray-dried from other carbohydrate solutions[16, 17]. The surface coverage of protein can be reduced by increasing viscosity[133] of the spray solution, but this is unlikely the case here.

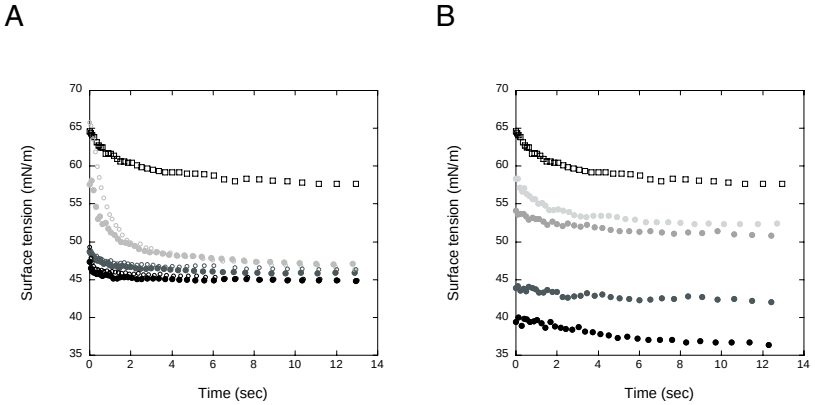

Figure 24. Dynamic surface tension of solutions with BSA and trehalose (squares) after addition of increasing amounts (indicated by darker spots) of (A) 0.1%; 1%; and 9.9% HPMC of dry weight, and (B) 0.1%; 1%; 9.9% and 26% poloxamer of dry weight. Polymer/trehalose only (unfilled), protein/poymer/trehalose (filled).

At a polymer concentration of approximately 10% w/w of dry weight the polymer coverage was 30% higher with HPMC compared to poloxamer (Fig. 25). Even at concentrations as high as 26% w/w of dry weight poloxamer (not shown) the percentage of polymer at the surface was lower compared to that of 10% w/w of HPMC. This can presumable be explained by the poloxamer forming a thinner film than HPMC, thus the ESCA signal is a combination of a (resonably) complete surface film of poloxamer and the underlaying material containing carbohydrate as well as protein. Interestingly, no signal was detected from the protein. This might indicate a steric effect from the adsorbed poloxamer layer, with the PEO-tails pointing towards the solution at higher concentrations[89, 131]. Thereby, globular BSA but not trehalose might be excluded from the (sub) surface layer. The suppression of BSA from the surface in spray-dried particles, by addition of polymer, was illustrated by CLSM (Fig. 26)

A

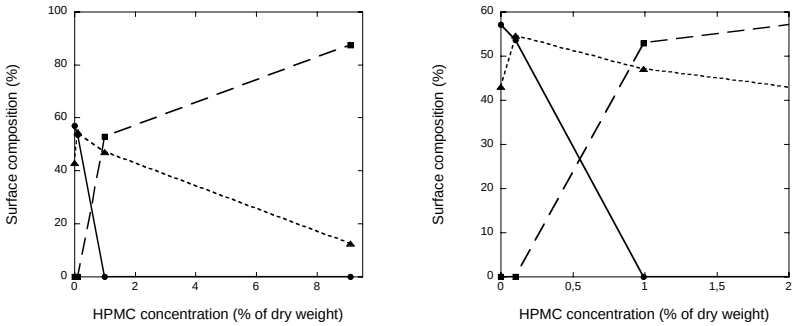

B

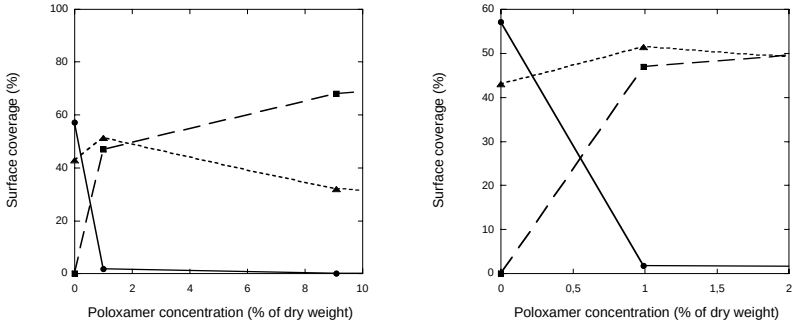

Figure 25. Surface composition estimated by ESCA as a function of the polymer concentration. (A) HPMC and (B) poloxamer. BSA (●), trehalose (▲), and (■) polymer. Range 0–9.9% w/w (left) and 0–1% w/w (right)

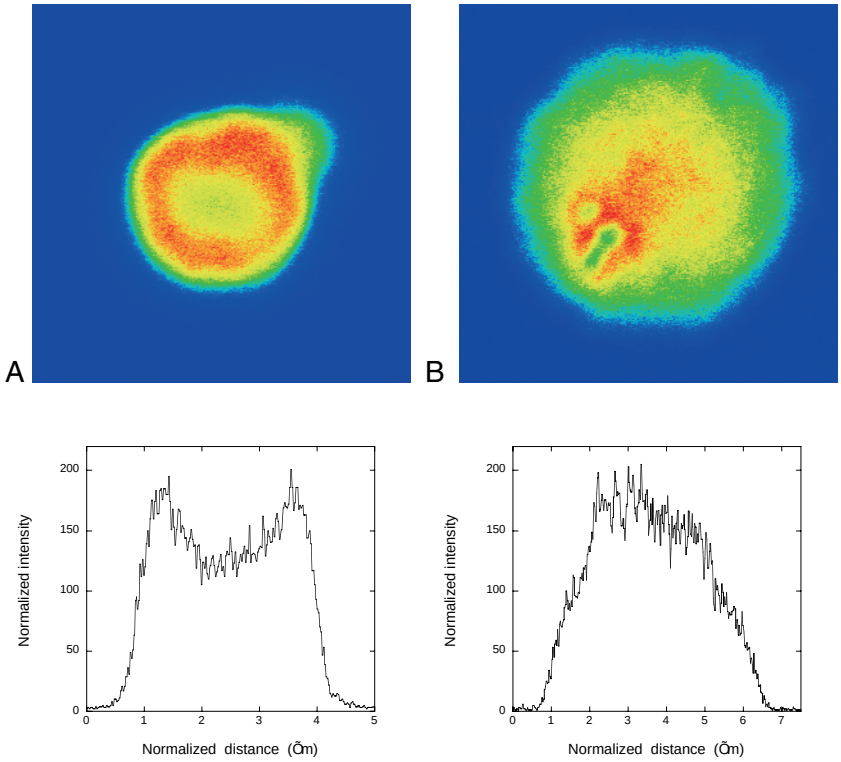

Figure 26. CLSM cross-sections illustrating the distribution of FITC-BSA in a particle before (A) and after (B) in situ coating. The distribution is correlated to the intensity showed in the profile underneath.

The surface composition influences the particle size, shape and surface morphology

It is reasonable to believe that the chemical composition of the particle surface will affect particle properties, such as dissolution and flowability. Similarly, particle formation will depend on solute properties, as described in Paper I and II. In addition, Paper V highlights the significance of the chemical surface composition during spray drying. Inclusion of polymeric materials, even at low concentrations, changed the particle surface morphology substantially (Fig. 27). Similarly to what was reported on the ATPS particles in Paper IV, the corrugated morphology caused by the cohesive protein film turned into a spherical particle with a smooth surface by preferential adsorption poloxamer (Fig. 27). In contrast, HPMC appeared to form a similar type of film as proteins, since the particle morphology was affected in a similar way as for protein containing particles. Data on surface viscosity found in literature verified this hypothesis, and it was possible to rank the polymers used in this thesis according to their flexibility and surface visco-elasticity. For example, the elastic modulus (G´) of HPMC was 130 mN/m[134] whereas

the dilatational modulus (E) of both PVA and poloxamer was comparatively lower, 11 mN/m[128] and 2 mN/m[89], respectively. Consequently, with a dilatational modulus of approximately 60 mN/m[128, 129] this places BSA between HPMC and PVA. In addition, low-molecular surfactants, such as polysorbates as very mobile and hence, without surface elasticity, which may explain the observations of smooth spheres after addition of *e.g.* polysorbate.[50, 52]

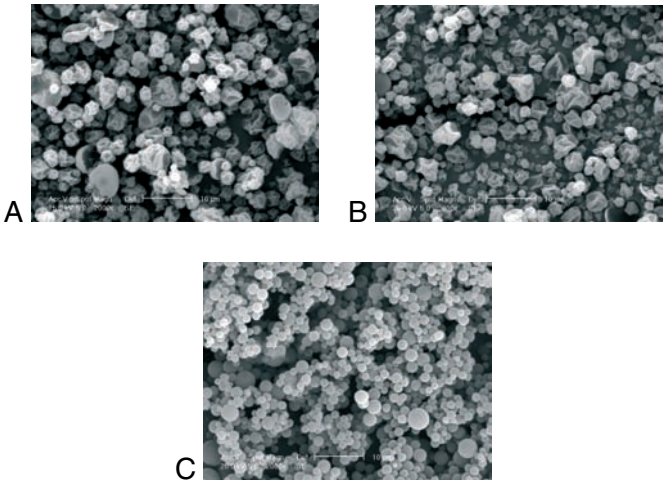

Figure 27. The morphology of spray-dried in situ coated particles were affected by the type of coating. (A) uncoated; (B) HPMC; and (C) poloxamer. Bar lenght 10 μm.

~~S~~tudies with gas pycnometry, showed a correlation between the polymer concentration and the apparent particle density of the spray-dried powder (Table 5). However, the effect was considerably more pronounced with the HPMC coating compared to the poloxamer coating, possibly due to HPMC forming a thicker film. Similar reductions in the apparent particle density with increasing concentration of polymer were observed for the ATPS in Paper IV and it is likely that the reduction in apparent particle density, by gas pycnometry, is related to the gas permeability of the particle surface.

Table 5. The apparent density, by gas pycnometry, of *in situ* coated particles. Mean value, SD<0.006 (n=10)

Polymer (% dry weight)	BSA/Trehalose/ HPMC (g/cm^3)	Trehalose/HPMC (g/cm^3)	BSA/Trehalos/ poloxamer (g/cm^3)
0	1.51	1.54	1.51
0.1	1.50	1.53	1.49
1.0	1.46	1.47	1.48
9.9	1.23	1.24	1.43
26	–	–	1.41

A possible application for *in situ* coated particles is for a modified release purpose. Although the amount of polymer is low compared to conventional coatings, a three-fold increase of the dissolution time was observed in the concentration span investigated here (Fig. 28). Apparently, the dissolution time depended on the surface coverage of HPMC rather than the concentration in the bulk (Fig. 28).

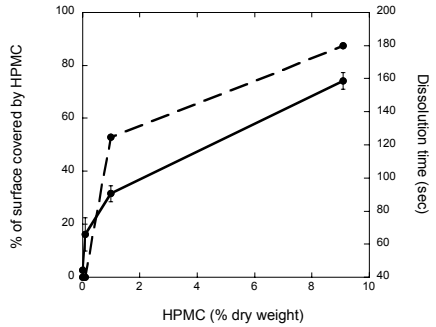

Figure 28. Dissolution time as a function of total polymer concentration and surface coverage.

Interestingly, better flow properties of particles coated with poloxamer compared to HPMC were noticed during spray drying and powder handling. Possibly, interparticulate interactions were affected by either surface composition or particle shape and morphology.[135] For example, the water sorption isotherm of poloxamer is below that of HPMC[25], resulting in a less "sticky" powder. However, it was not possible to confirm these results by flowability tests and close inspections of SEM images implied that the primary particles in samples with high poloxamer content were agglomerated into small aggregates, which may in part account for the improved flow properties.

Inclusion of polymeric material can influence the re-crystallization behavior of *e.g.* spray-dried lactose.[136-138] However, *in situ* coating by HPMC or poloxamer did not change the T_g of the formulations, at least not for the concentrations studied here. Further, all samples coated with HPMC were amorphous. In contrast, particles coated with poloxamer showed the presence of crystalline polymer, with a melting transition at approximately 50–53°C (Paper V). Apparently, the addition of a surface-active polymer, such as HPMC or poloxamer result in phase separation during spray drying, due to the surface activity of the polymer and the mixing of polymer and trehalose is limited. In contrast, addition of *e.g.* dextran, which has no surface activity, forms amorphous particles, with a T_g dependant of the mass content of each excipient (Paper IV).

Structural integrity of BSA in *in-situ* coated particles

From the extensive investigation of BSA conformation in the dried and rehydrated state it was concluded that all formulations had a native-like conformation and hence, addition of low contents of non-ionic polymers, such as HPMC or poloxamer, can help preserve or reduce surface induced destabilization. Neither was any unfavorable interaction between the protein and polymer found, as observed between BSA and PVA in spray-dried ATPS (Paper IV). However, the structural integrity was also high in uncoated particles which indicate that the stabilization of BSA observed here is mostly due to trehalose. Approximately 4% of the total content of protein can be expected at the particle surface at a protein concentration of 5% w/w in the powder.[17, 90] Possibly, the small increase of α-helix content from 43% to 47% on average and the modest increase of monomer from 88% to 89% can be attributed to the decreased surface levels of protein during drying (Table 7). In comparison, both α-helix and monomer content was substantially decreased (33% and 34%, respectively) as BSA was spray-dried from a fomulation with 80% less trehalose (Table 7). It is likely that a lower protein concentration in the spray solution would have resulted in a higher adsorbed fraction of protein at the droplet surface[17, 90], and possibly a significant as well as concentration dependent effect of the *in situ* coating. However, due to the limitations regarding the protein concentration needed for liquid FTIR, the protein concentration of the spray solutions was set to 5 mg/ml.

Table 6. Structural integrity of protein in *in situ* coated particles. The total solids content was 10% w/w.

Excipients	Polymer (% of dry weight)	Protein: Sugar mass ratio	CD	FTIR α-helix content (%)	Gel filtration N=native BSA, Aggr=soluble aggregates (insoluble), Frag=fragments (%)		
				α	N	Aggr	Frag
BSA, native	-	-	N	55	89	11	-
Dextran, trehalose	-	1:3.8	-	33	34	2 (13)	51
Trehalose	0	1:19	N	43	88	12	-
HPMC, trehalose	0.1	1:19	N	49	89	11	-
	1.0	1:19	N	45	89	11	-
	9.9	1:19	N	47	89	11	-
Poloxamer, trehalose	0.1	1:19	na	na	86	14	-
	1.0	1:19	N	na	89	11	-
	9.9	1:19	N	na	na	na	na
	26	1:19	N	na	na	na	na

Summary and conclusions

Particle formation during spray drying

Conclusively, this thesis has made some important additions to the knowledge on particle formation, related to size, density and surface composition of individual particles, during spray drying. The first part of the thesis, described drying of simple carbohydrate systems of relevance to pharmaceutical preparations (Paper I-III). The acquired knowledge is applicable to inhalation powders, where control of size and density of individual particles is required. First, several ways of changing the particle size during spray drying were presented. Earlier it has not been clear how conditions during atomization, and the type and concentration of the excipients interact and control the properties of the particles. For example, the particle size was predictable from data on droplet size, yield and the solubility of the solute at the wet bulb temperature during spray drying (Paper II). Second, this thesis touches upon the possibility to control the density of spray-dried particles, by process or by choice of excipients. Formation of different internal structures was found to depend on the propensity of the carbohydrate to crystallize during spray drying (Paper II). This hypothesis, suggested in Paper II, on the formation of hollow and porous particles, was supported by measurements of droplet size before and after drying and by measurements of the apparent particle density of spray-dried powders with different solid concentrations (Paper I-II). Further, the different types of internal structures were illustrated by various microscopy techniques (SEM, TEM, CLSM and light microscopy) showing cross-sections of particles (Paper 1-III). Finally, an AFM method for the assessment of the effective density of single particles confirmed the presence of different internal structures in materials with different crystallizing propensity (Paper III).

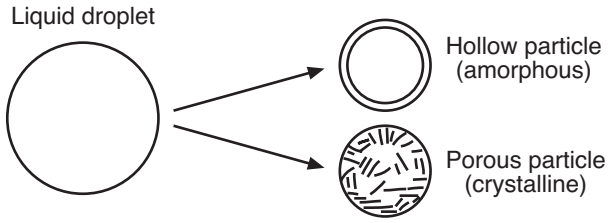

Figure 28. Schematic illustration of the formation of hollow and porous particles during spray drying.

Protein stabilization during spray drying

In the second part of this thesis, two new formulation concepts using non-ionic polymers for encapsulation and coating of protein formualations during spray drying were evaluated. The effect of the competitive surface adsorption during atomization and drying on the protein stability, surface composition, as well as particle properties were demonstrated.

First, the formulation concept using ATPSs of the non-ionic polymers PVA and dextran, proved to be very efficient for encapsulation of BSA (Paper IV). However, a specific interaction between BSA and PVA counteracted the expected protective effect of the ATPS. Nevertheless, a possible application for the ATPS concept could be for *e.g.* controlled release formulations. By proper choice of polymers, control of droplet size (of the dispersed phase) and behavior upon reconstitution various wetting and dissolution profiles, (related to the surface composition), may be obtained.

Second, two other non-ionic polymers, HPMC and poloxamer 188, selected due to their presumed different adsorption kinetics and surface rheology during spray drying, both proved efficient for *in situ* coating of protein containing particles, even at low concentrations (Paper V). BSA was repressed from the particle surface by addition of typically 1 % w/w polymer of dry weight. Changes in the particle surface morphology, induced by the addition of the polymer, were correlated to the chemical composition of the particle surface and presumably by the surface rheology at the droplet surface during drying. Other particle properties, such as, dissolution, powder flowability and apparent particle density could also be assigned to the coating efficiency. The formulation concepts presented in this thesis may be particularly suitable to low-dosage formulations where a substantial surface induced denaturation of protein can be expected.

Future directions

Of particular interest and surprise to me has been the distinction in the formation of hollow and porous particles in amorphous and crystalline carbohydrate particles, respectively. As evident from the AFM measurements of the effective density the hollow particles occurred together with solid particles while no solid particles were found in the samples with porous particles. One may wonder if the degree of "porosity" can be affected by addition of a component affecting the recrystallization during spray drying. For example polymers, such as PVP and PEG have been reported to influence the recrystallization of spray-dried lactose.[136-138] The AFM method enables an estimation of the effective particle density and whether particles are hollow or porous.

It would also be very interesting to further investigate the relationship between the droplet surface rheology and the particle morphology. As suggested in Paper V corrugated particles can turn into smooth spheres if the component adsorbing to the surface during drying has a low surface viscosity compared to the component causing the cohesive film. To challenge this, and possibly understand the underlying mechanisms, would include analysis of (bulk and surface) diffusion, adsorption kinetics and surface rheology in protein and polymer mixtures. Likely surface composition will also depend on the molecular weight and degree of substitution of the polymer.

One may also ask oneself: how extensive is the surface induced destabilization of proteins, in comparison with the conformational stress induced by drying? Likely, the relation between the extent of surface and bulk destabilization will depend on the concentration of the protein. In low-dosage forms with a high fraction of the protein adsorbed to the air/water interface, possibly a variation in the surface viscosity between proteins might result in a varying degree of wrinkled surface during drying and hence the total surface area avialable for protein denaturation. Adsorption isotherms, dynamic surface tension (milliseconds region) combined with chemical surface analysis after drying and analysis of protein integrity may be helpful here.

Last but not least, both the particle formation and the surface composition[139] may depend on the drying rates, during spray drying, and hence, studies on the influence of drying conditions can be included in the above mentioned investigational areas.

Acknowledgements

The studies in this thesis were performed at YKI, Institute for Surface Chemistry (YKI, Ytkemiska Institutet AB), Stockholm, Sweden.

I wish to express my gratitude to AstraZeneca R&D, Lund, Sweden for financial support of this PhD-project. Further, IF Foundation, Swedish Academy of Pharmaceutical Sciences is acknowledged for the student grant facilitating a research stay at University of Colorado Health Science Centre (UCHSC), Denver, Colorado.

I would like to express my sincere gratitude to my supervisors:
Dr. Anna Millqvist-Fureby at YKI, my head supervisor, for your vast knowledge in protein drying and great interest in my projects. Thanks for all your suggestions, your help in preparing manuscripts and for many fruitful discussions on everything from the Molier chart to formula.
Dr. Ulla Elofsson at YKI, my supervisor during the first year. Thank you for accepting me and the project at YKI and for your helpfulness.
Prof. Göran Alderborn at the department of Pharmacy, Uppsala University, my second supervisor, for accepting me as your student and for thoughtful comments to my results.
Dr. Hans Karlsson, AstraZeneca R&D Lund, project industry representative, for "co-supervison" and industrial aspects to results presented at numerous meetings.

I am also grateful to many other persons who made some parts of this thesis possible to perform:
Prof. John F Carpenter (UCHSC) for allowing me to spend some weeks in his laboratory learning FTIR. Former and present PhD students in the lab: Shouvik, Krishnan, Kim-Sung, Tia and Derrick for teaching me FTIR, dragging nitrogen tubes, for SEC-HPLC, for the fan, excursions and friendship.

Dr. Karin M Andersson, Sandvik Tooling FoU, co-author and AFM maestro in Paper III–a good collaboration on the mysteries within.

At AstraZeneca R&D Lund & Södertälje: Dr. Stefan Ulvenlund for letting me run some CD; Dr. Kyrre Thalberg and Dr. Mårten Svensson for explorative powder characterization; Dr. Lars-Erik Briggner for valuble comments

on solid-state analysis; Dr. Ingvar Ymén for help with refractive indeces. Dr. Per Broberg for your enthusiasm to my statistical concerns and for your friendship; Inga Elding, librarian, for continuous update on search profiles. My former co-workers in the "tablet-group" Lars Nyborg, Lasse Leander and Lewi Lundgren and the other ex-AZ OFIR-members: Kristina Thyresson, Helena Eklöf, and Dr. Anette Seo for your kind interest and support.

Dr. Andres Valdes and Lic. Ulrika Eriksson for the use of your ÄKTA gel filtration equipment.

Dr. Marco van de Weert at the Danish Pharmaceutical University for kindly answering to questions on FTIR

Susanne Möllman, DFU and other co-workers in the ELF-project.

Moreover I thank all fellow PhD students at YKI (and FSFG) for friendship and good times, especially my present and former room mates: Tobias Halthur and Andreas Sonesson. "Without the two of you the room would definitely have had a different atmosphere"; my pharmacist-fellow Dr. Brita Rippner-Blomqvist; Torbjörn Pettersson and Joakim Voltaire. Super-thanks to Tobias for .epsarna and Andreas and Nina for CLSM and TEM, respectively. Satyan Gohil for his diploma work on sucrose.

My co-workers in the Pharmaceuticals and Foods Section and other colleagues at YKI, especially Rodrigo Robinson, Annika Olsson, Britt Nyström, Mikael Sundin and Karin Hallstensson for your helpfulness.

Former and present PhD students at galeniken in Uppsala, whom I have hade the pleasure to meet and travel with.

Thank you all other friends outside YKI for contributing to my life with others besides spray drying. Malin, Lilianne, Skåne-tjejerna, Ängelholmarna, my special "mamma-friends" Åsa and Lotti, Omstart… I miss you all and I long to spend some time with you again.

Thanks also to my family for your support and concerns: My dear mum Ullabritt, my sister Sara–"I owe you a lot of baby-sitting one day…", Johan M, Emma & Marcus, Matilda, Lena and Kalle.

My best friend, my companion and love–Johan. Thanks for taking so good care of me, our daughter and everything else during this hectic time. Ella, "min lilla tjej–nu vill jag hem å krama dej…"

References

1 Patton, J. S. and Platz, R. M. 1992. Pulmonary delivery of peptides and proteins for systemic action. Adv. Drug Deliv. Rev. 8:179-196.

2 Wall, D. A. 1995. Pulmonary absorption of peptides and proteins. Drug Deliv. 2(1):1-20.

3 Hickey, A. J., Martonen, T. B. and Yang, Y. 1996. Theoretical relationship of lung deposition to the fine particle fraction of inhalation aerosols. Pharm. Acta Helv. 71(3):185-190.

4 Schulz, H. 1998. Mechanisms and factors affecting intrapulmonary particle deposition: implications for efficient inhalation therapies. PSTT 1(8):336-344.

5 Crowder, T. M., Rosati, J. A., Schroeter, J. D., Hickey, A. and Martonen, T. B. 2002. Fundamental effects of particle morphology on lung delivery; predictions of Stoke´s law and the particlular relevance to dry powder inhaler formulation and development. Pharm. Res. 19(3):239-245.

6 Salekigerhardt, A., Ahlneck, C. and Zografi, G. 1994. Assessment of Disorder in Crystalline Solids. Int. J. Pharm. 101(3):237-247.

7 Vanbever, R., Mintzes, J. D., Wang, J., Nice, J., Chen, D. H., Batycky, R., Langer, R. and Edwards, D. A. 1999. Formulation and physical characterization of large porous particles for inhalation. Pharm. Res. 16(11):1735-1742.

8 Edwards, D. A., Hanes, J., Caponetti, G., Hrkach, J., Ben-Jebria, A., Eskew, M. L., Mintzes, J., Deaver, D., Lotan, N. and Langer, R. 1997. Large porous particles for pulmonary drug delivery. Science 276(5320):1868-1871.

9 French, D. L., Edwards, D. A. and Niven, R. W. 1996. The influence of formulation on emission, deaggregation and deposition of dry powders for inhalation. J. Aerosol Sci. 27(5):769-783.

10 Li, W. I. and Edwards, D. A. 1997. Aerosol particle transport and deaggregation phenomena in the mouth and throat. Adv. Drug Deliv. Rev. 26(1):41-49.

11 Warheit, D. B. and Hartsky, M. A. 1993. Role of alveolar macrophage chemotaxis and phagocytosis in pulmonary clearance responses to inhaled particles: Comparisons among rodent species. Microsc. Res. Tech. 26(5):412-422.

12 Hardy, J. G. and Chadwick, T. S. 2000. Sustained Release Drug Delivery to the lungs. Clinical Pharmacokinetics 39(1):1-4.

13 Maa, Y. F., Nguyen, P. A., Sit, K. and Hsu, C. C. 1998. Spray-drying performance of a bench-top spray dryer for protein aerosol

powder preparation. Biotechnology and Bioengineering.60(3):301-309.
14 Mosén, K., Backstrom, K., Thalberg, K., Schaefer, T., Kristensen, H. G. and Axelsson, A. 2004. Particle formation and capture during spray drying of inhalable particles. Pharm. Develop. Technol. 9(4):409-417.
15 Masters, K. 1991. Spray drying handbook. 5th ed., Harlow: Longman Scientific & Technical.
16 Fäldt, P. and Bergenståhl, B. 1994. The surface composition of spray-dried protein-lactose powders. Coll. Surf. A 90:183-190.
17 Landström, K., Alsins, J. and Bergenståhl, B. 2000. Competitive protein adsorption between bovine serum albumin and β-lactoglobulin during spray-drying. Food Hydrocolloids 14:75-82.
18 Millqvist-Fureby, A., Malmsten, M. and Bergenståhl, B. 1999. Spray-drying of trypsin - surface characterisation and activity preservation. Int. J. Pharm. 188:243-253.
19 Fäldt, P. and Bergenståhl, B. 1993. The surface coverage of fat on food powders analyzed by ESCA (electron spectroscopy for chemical analysis). Food Structure 12:225-234.
20 Filkova, I. and Cedlik, P. 1984. Nozzle atomization in spray drying. Advances in Drying 3:181-215.
21 Lefebvre, A. H. 1989. Atomization and Sprays. New York: Hemispere Publishing Corporation. p 421.
22 Nukiyama, S. and Tanasawa, Y. 1938. An experiment on the atomization of liquid by means of an air stream. Trans Soc Mech Engrs (Japan) 4/5:13-17.
23 Masters, K. 1994. Spray drying handbook. 5th ed., New York: Longman Scientific & Technical. p 193-274.
24 Kim, K. Y. and Marshall, W. R. 1971. Amer Inst Chem Eng J 17(3):5757.
25 Kibbe, A. 2000. Handbook of pharmaceutical excipients. 3rd ed., New York: American Pharmaceutical Association and Pharmaceutical Press.
26 Snoeren, T. H. M., Damman, A. J., Klok, H. J. and van Mil, P. J. J. M. 4th International Drying Symposium, 1984, pp 358-363.
27 Dexter, R. W. 1996. Measurement of extensional viscosity of polymer solutions and its effects on atomization from a spray nozzle. Atomization and Sprays 6(2):167-191.
28 Harrison, G. M., Mun, R., Cooper, G. and Boger, D. V. 1999. A note on the effect of polymer rigidity and concentration on spray atomisation. Journal of Non-Newtonian Fluid Mechanics 85(1):93-104.
29 Millqvist-Fureby, A., Malmsten, M. and Bergenståhl, B. 2000. An aqueous polymer two-phase system as carrier in spray-drying of biological material. J. Colloid Interface Sci. 225(1):54-61.
30 Filková, I. 1991. Spray drying of non-newtonian liquids. In Mujumdar, A. S. and Filková, I., editors. Drying ´91, ed., New York: Elsevier Science Publishers B. V. p 632.

31 Dexter, R. W. and Huddleston, E. W. 1998. Effects of adjuvants and dynamic surface tension on spray properties under simulated aerial conditions. ASTM STP 1347:95-106.
32 Dunbar, C. A., Concessio, N. M. and Hickey, A. J. 1998. Evaluation of atomizer performance in production of respirable spray-dried particles. Pharm. Develop. Technol. 3(4):433-441.
33 Fell, J. T. and Newton, J. M. 1971. The production and properties of spray dried lactose: part 2. Pharm. Acta Helv. 46:425-430.
34 Cassidy, O. E., Carter, P. A., Rowley, G. and Merrifield, D. R. 2000. Triboelectrification of Spray-dried Lactose Prepared from Different Feedstock Concentrations. J. Pharm. Pharmacol. 52:13-17.
35 van Mil, P. J. J. M., Hols, G. and Klok, H. J. 1988. Spray drying of concentrated milk: relation between initial droplet size and fine particle size. In Bruin, S., editor Preconcentration and Drying of Food Materials, ed., Amsterdam: Elsevier Science Publishers B. V. p 193-202.
36 Marshall, W. R. J. 1954. Atomization and spray drying. New York: The Science Press.
37 Chawla, J. M. 1994. Effect of the droplet agglomeration on the design of spray dryer towers. Dry. Technol. 12(6):1357-1365.
38 Pérez-Correa, J. R. and Farías, F. 1995. Modelling and control of a spray dryer: a simulation study. Food Control 6(4):219-227.
39 Adhikari, B., Bhandari, B. R. and Troung, V. 2000. Experimental studies of single drop drying and their relevance in drying of sugar-rich foods: a review. Int. J. Food Prop. 3(3):323-351.
40 Hassan, H. M. and Mumford, C. J. 1996. Mechanisms of drying of skin-forming materials; The significance of skin formation and a comparison between three types of material. Dry. Technol. 14(7-8):1763-1777.
41 Greenwald, C. G. and King, C. J. 1982. The mechanism of particle expansion in spray drying of foods. Food Proc. Eng. 78:101-110.
42 Alexander, K. 1983. Factors governing surface morphology in the spray-drying of foods. Ph.D. Thesis. University of California. Berkely, CA.
43 Elsayed, T. M., Wallack, D. A. and King, C. J. 1990. Changes in particle morphologyduring drying of drops of carbohydrate solutions and food liquids .1. Effects of composition and drying conditions. Ind. Eng. Chem. Res. 29(12):2346-2354.
44 Meerdink, G. 1993. Drying of Liquid Food Droplets: Enzyme Inactivation and Multicomponent diffusion. Ph.D. Thesis. Agricultural University Wageningen. Wageningen.
45 Swithenbank, J., Beer, J. M., Taylor, D. S., Abbot, D. and C., M. C. G. 1977. A laser diagnostic technique for the measurement of droplet and particle size distribution. In Zinn, B. T., editor Experimental Diagnostics in Gas Phase Combustion Systems, ed.: American Institute of Aeronautics and Astronautics. p 421-447.

46 Kufferath, A., Wende, B. and Leuckel, W. 1999. Influence of liquid flow conditions on spray characteristics of internal-mixing twin-fluid atomizers. Int. J. of Heat and Fluid Flow 20(5):513-519.
47 Absolom, D. R., Van Oss, C. J., Zingg, W. and Neumann, A. W. 1981. Determination of surface tension of proteins II. Surface tension of serum albumin at the protein air interface. Biochim. Biophys. Acta 670:74-78.
48 Norde, W. and Giacomelli, C. E. 2000. BSA structural changes during homomolecular exchange between the adsorbed and the dissolved states. Journal of Biotechnology 79(3):259-268.
49 Mumenthaler, M., Hsu, C. C. and Pearlman, R. 1994. Feasibility study on spray-drying protein pharmaceuticals: recombinant human growth hormone and tissue-type plaminogen Activator. Pharm. Res. 11(1):12-20.
50 Maa, Y. F., Nguyen, P. A. T. and Hsu, S. W. 1998. Spray-drying of air-liquid interface sensitive recombinant human growth hormone. J. Pharm. Sci. 87(2):152-159.
51 Broadhead, J., Rouan, S. K. E., Hau, I. and Rhodes, C. T. 1994. The effect of process and formulation variables on the properties of spray-dried beta-galactosidase. J. Pharm. Pharmacol. 46(6):458-467.
52 Adler, M., Unger, M. and Lee, G. 2000. Surface composition of spray-dried particles of bovine serum albumin/trehalose/surfactant. Pharm. Res. 17(7):863-870.
53 Andrade, J. D. and Hlady, V. 1986. Protein adsorption and materials biocompatibility: A tutorial review and suggested hypotheses. Advances in Polymer Science 79:1-63.
54 Millqvist-Fureby, A., Burns, N., Landström, K., Fäldt, P. and Bergenståhl, B. 1999. Surface ctivity at the air-water interface in relation to surface composition of spray-dried milk protein-stabilized emulsions. In Rodríguez Patino, J. M., editor Food emulsions and foams - Interfaces, interactions and stability, ed., Cambridge: The Royal Society of Chemistry. p 236-245.
55 Blomberg, E., Claesson, P. M., Froberg, J. C. and Tilton, R. D. 1994. Interaction between adsorbed layers of Lysozyme studied with the surface force technique. Langmuir 10(7):2325-2334.
56 Landström, K. 2000. Competitive protein adsorption during spray-drying. Ph.D. Thesis. Lund University. Lund.
57 Nasir, A. and McGuire, J. 1998. Sequential and competitive adsorption of bovine serum albumin and beta-lactoglobulin, and their resistance to exchange with alpha-lactalbumin and beta-casein. Food Hydrocolloids 12(1):95-103.
58 Wahlgren, M. C., Paulsson, M. A. and Arnebrant, T. 1993. Adsorption of globular model proteins to silica and methylated silica surfaces and their elutability by dodecyltrimethylammonium bromide. Colloids and Surfaces a-Physicochemical and Engineering Aspects 70(2):139-149.

59 Tripp, B. C., Magda, J. J. and Andrade, J. D. 1995. Adsorption of globular-proteins at the air/water interface as measured via dynamic surface-tension - Concentration-dependence, mass-transfer considerations, and adsorption-kinetics. J. Colloid Interface Sci. 173(1):16-27.

60 Frokjer, S. and Hovgaard, L. editors. 2000. Pharmaceutical formulation and development of peptides and proteins. London: Taylor & Francis. p 1-238.

61 Carpenter, J. F. and Manning, M. C. editors. 2002. Rational design of stable protein formulations. Theory and practise. New York: Kluwer Academic. p 1-203.

62 Wang, W. 2005. Protein aggregation and itss inhibition in biopharmaceutics. International Journal of Pharmaceutics 289:1-30.

63 Arakawa, T., Prestrelski, S. J., Kenney, W. C. and Carpenter, J. F. 1993. Factors affecting short-term and long-term stability of proteins. Advanced Drug Delivery Reviews 10:1-28.

64 Timasheff, S. N. 1992. Water as ligand - Preferential binding and exclusion of denaturants in protein unfolding. Biochemistry 31(41):9857-9864.

65 Timasheff, S. N. 1993. The control of protein stability and association by weak-interactions with water - How do solvents affect these processes. Annual Review of Biophysics and Biomolecular Structure 22:67-97.

66 Carpenter, J. F. and Crowe, J. H. 1988. The mechanism of cryoprotection of proteins by solutes. Cryobiology 25:244-255.

67 Green, J. L. and Angell, C. A. 1989. Phase-relations and vitrification in saccharide-water solutions and the trehalose anomaly. J. Phys. Chem. 93(8):2880-2882.

68 Franks, F., Hatley, R. H. M. and Mathias, S. F. 1991. Materials science and the production of shelf-stable biologicals. BioPharm 4(9):38-55.

69 Belton, P. S. and Gil, A. M. 1994. IR and Raman spectroscopic studies of the interaction of trehalose with hen egg white lysozyme. Biopolymers 34:957-961.

70 Costantino, H. R., Langer, R. and Klibanov, A. M. 1994. Solid-phase aggregation of proteins under pharmaceutically relevant conditions. J. Pharm. Sci. 83(12):1662-1669.

71 Pikal, M. J. and Rigsbee, D. R. 1997. The stability of insulin in crystalline and amorphous solids: Observation of greater stability for the amorphous form. Pharm. Res. 14(10):1379-1387.

72 Costantino, H. R., Andya, J. D., Nguyen, P. A., Dasovich, N., Sweeney, T. D., Shire, S. J., Hsu, C. C. and Maa, Y. F. 1998. Effect of mannitol crystallization on the stability and aerosol performance of a spray-dried pharmaceutical protein, recombinant humanized anti-IgE monoclonal antibody. J. Pharm. Sci. 87(11):1406-1411.

73 Adler, M. and Lee, G. 1999. Stability and surface activity of lactate dehydrogenase in spray dried trehalose. J. Pharm. Sci. 88(2):199-208.
74 Tzannis, S. T. and Prestrelski, S. J. 1999. Activity-stability considerations of trypsinogen during spray drying: Effects of sucrose. J. Pharm. Sci. 88(3):351-359.
75 Carpenter, J. F. and Crowe, J. H. 1989. An infrared spectroscopic study of the interactions of carbohydrates with dried proteins. Biochemistry 28:3916-3922.
76 Prestrelski, S. J., Tedeschi, N., Arakawa, T. and Carpenter, J. F. 1993. Dehydration-induced conformational transitions in proteins and their inhibition by stabilizers. Biophysical Journal 65:661-671.
77 Allison, S. D., Chang, B., Randolph, T. W. and Carpenter, J. F. 1999. Hydrogen bonding between sugar and protein is responsible for inhibition of dehydration-induced protein unfolding. Arch. Biochem. Biophys. 365(2):289-298.
78 Pikal, M. J., Dellerman, K. M., Roy, M. L. and Riggin, R. M. 1991. The Effects of Formulation Variables on the Stability of Freeze-Dried Human Growth-Hormone. Pharm. Res. 8(4):427-436.
79 Kreilgaard, L., Frokjaer, S., Flink, J. M., Randolph, T. W. and Carpenter, J. F. 1999. Effects of additives on the stability of Humicola lanuginosa lipase during freeze-drying and storage in the dried solid. J. Pharm. Sci. 88(3):281-290.
80 Allison, S. D., Manning, M. C., Randolph, T. W., Middleton, K., Davies, A. and Carpenter, J. F. 2000. Optimization of storage stability of lyophilized actin using combinations of disaccharides and dextran. J. Pharm. Sci. 89(2):199-214.
81 Imamura, K., Fukushima, A., Sakaura, K., Sugita, T., Sakiyama, T. and Nakanishi, K. 2002. Water sorption and glass transition behaviors of freeze-dried sucrose-dextran mixtures. J. Pharm. Sci. 91(10):2175-2181.
82 Tanaka, K., Takeda, T. and Miyajima, K. 1991. Cryoprotective Effect of Saccharides on Denaturation of Catalase by Freeze-Drying. Chemical & Pharmaceutical Bulletin 39(5):1091-1094.
83 Cleland, J. L., Lam, X., Kendrick, B., Yang, J., Yang, T. H., Overcashier, D., Brooks, D., Hsu, C. and Carpenter, J. F. 2001. A specific molar ratio of stabilizer to protein is required for storage stability of a lyophilized monoclonal antibody. J. Pharm. Sci. 90(3):310-321.
84 Imamura, K., Suzuki, T., Kiril, S., Tatsumichi, T. and Okazaki, M. 1998. Influence of protein on phase transition of amorphous sugar. Journal of Chemical Engineering of Japan 31(3):325-329.
85 Hancock, B. C., Shamblin, S. L. and Zografi, G. 1995. Molecular Mobility of Amorphous Pharmaceutical Solids Below Their Glass-Transition Temperatures. Pharm. Res. 12(6):799-806.
86 Duddu, S. P., Zhang, G. Z. and DalMonte, P. R. 1997. The relationship between protein aggregation and molecular mobility below the

glass transition temperature of lyophilized formulations containing a monoclonal antibody. Pharm. Res. 14(5):596-600.
87 Ledl, F. and Schleicher, E. 1990. New Aspects of the Maillard Reaction in Foods and in the Human-Body. Angewandte Chemie-International Edition in English 29(6):565-594.
88 Bhattacharya, A. and Ray, P. 2004. Studies on surface tension of poly(vinyl alcohol): Effect of concentration, temperature, and addition of chaotropic agents. J. Appl. Polymer Sci. 93(1):122-130.
89 Blomqvist, B. R., Warnheim, T. and Claesson, P. M. 2005. Surface rheology of PEO-PPO-PEO triblock copolymers at the air-water interface: Comparison of spread and adsorbed layers. Langmuir 21(14):6373-6384.
90 Landström, K., B, B., Alsins, J. and Almgren, M. 1999. A fluorescens method for quantitative measurements of specific protein at powder surfaces. Coll. Surf. B 12:429-440.
91 British standards institution Glossary of terms relating to powders. 1958. London: British standards institution. p 1-16.
92 Christensen, K. L., Pedersen, G. P. and Kristensen, H. G. 2001. Preparation of redispersible dry emulsions by spray drying. Int. J. Pharm. 212:187-194.
93 Wikberg, M. and Alderborn, G. 1992. Compression characteristics of granulated materials .6. Pore-size distributions, assessed by mercury penetration, of compacts of two lactose granulations with different fragmentation propensities. Int. J. Pharm. 84(2):191-195.
94 Andersson, K. M. and Bergström, L. 2005. Density measurements of single granules using the atmoic force microscope. J. Am.Ceram. Soc. 85(8):2322-2324.
95 Cleveland, J. P., Manne, S., Bocek, D. and Hansma, P. K. 1993. A nondestructive method for determining the spring constant of cantilevers for scanning force microscopy. Review of Scientific Instruments 64(2):403-405.
96 Briggs, D. and Grant, J. T. 2003. Surface analysis by Auger and X-ray photoelectron spectroscopy. Chichester: IM Publications and Surface Spectra Limited.
97 Briggs, D. and Seah, M. P. 1990. Practical surface analysis: Auger and X-ray photoelectron spectroscopy. 2nd ed., Chichester: Whiley.
98 Miller, R., Joos, P. and Fainerman, V. B. 1994. Dynamic Surface and Interfacial-Tensions of Surfactant and Polymer-Solutions. Advances in Colloid and Interface Science 49:249-302.
99 Fainerman, V. B., Miller, R. and Joos, P. 1994. The measurement of dynamic surface-tension by the maximum bubble pressure method. Colloid and Polymer Science 272(6):731-739.
100 Dong, A., Huang, P. and Caugney, W. S. 1990. Protein secondary structure in water from second.derivative amide I infrared spectra. Biochemistry 29:3303-3308.
101 Venyaminov, S. Y. and Prendergast, F. G. 1997. Water (H_2O and D_2O) molar absorptivity in the 1000-4000 cm^{-1} range and quantita-

tive infrared spectroscopy of aqueous solutions. Anal. Biochem. 248(2):234-245.
102 Zuber, G., Prestrelski, S. J. and Benedek, K. 1992. Application of Fourier-transform infrared-spectroscopy to studies of aqueous protein solutions. Anal. Biochem. 207(1):150-156.
103 van de Weert, M., Haris, P. I., Hennink, W. E. and Crommelin, D. J. A. 2001. Fourier transform infrared spectrometric analysis of protein conformation: Effect of sampling method and stress factors. Anal. Biochem. 297(2):160-169.
104 Srrerama, N. and Woody, R. W. 2000. Circular dichroism in peptides and proteins. In Berova, N., Nakanishi, K. and Woody, R. W., editors. Circular dichroism: principles and applications, 2nd ed., New York: John Whiley & Sons. p 601-620.
105 Soenderkaer, S., Carpenter, J. F., van de Weert, M., Hansen, L. L., Flink, J. and Frokjaer, S. 2004. Effects of sucrose on rFVIIa aggregation and methionine oxidation. Eur. J. Pharm. Sci. 21(5):597-606.
106 Heller, M. C., Carpenter, J. F. and Randolph, T. W. 1999. Protein formulation and lyophilization cycle design: Prevention of damage due to freeze-concentration induced phase separation. Biotechnol. Bioeng. 63(2):166-174.
107 Maa, Y. F. and Hsu, C. C. 1997. Protein denaturation by combined effect of shear and air-liquid interface. Biotechnol. Bioeng. 54(6):503-512.
108 Jouppila, K., Kansikas, J. and Roos, Y. H. 1998. Crystallization and X-ray diffraction of crystals formed in water-plasticized amorphous lactose. Biotechnol. Prog. 14(2):347-350.
109 Reiser, P., Birch, G. and Mahtlouthi, M. 1995. Physical properties. In Mathlouthi, M. and Reiser, P., editors. Sucrose Properties and applications, ed., Glasgow: Blackie Academic and Professional. p 186-222.
110 Sebhatu, T., Ahlneck, C. and Alderborn, G. 1997. The effect of moisture content on the compression and bond-formation of amorphous lactose particles. Int. J. Pharm. 146:101-114.
111 Weast, R. C. and Astle, M. J. 2000. CRC Handbook of data of organic compounds. ed., Boca Ranton: CRC Press.
112 Yu, L., Mishra, D. S. and Rigsbee, D. R. 1998. Determination of the glass properties of D-mannitol using sorbitol as an impurity. J. Pharm. Sci. 87(6):774-777.
113 Roos, Y. H. and Karel, M. 1990. Differential scanning calorimetry study of phase transitions affecting the quality of dehydrated materials. Biotechnol. Prog. 6:159-163.
114 McGarvey, O. S., Kett, V. L. and Craig, D. Q. M. 2003. An investigation into the crystallization of alpha,alpha-trehalose from the amorphous state. J. Phys. Chem. B 107(27):6614-6620.
115 Naini, V., Byron, P. R. and Phillips, E. M. 1998. Physicochemical stability of crystalline sugars and their spray-dried forms: Depend-

ence upon relative humidity and suitability for use in powder inhalers. Drug Dev. Ind. Pharm. 24(10):895-909.
116 Narasimhan, B., Snaar, J. E. M., Bowtell, R. W., S., M., Melia, C. D. and Peppas, N. A. 1999. Magnetic resonance imaging analysis of molecular mobility during dissolution of poly(vinyl alcohol) in water. Macromolecules 32:704-710.
117 Machiste, E. O. and Buckton, G. 1996. Dynamic surface tension of hydroxypropylmethylcellulose film-coating solutions. Int. J. Pharm. 145:197-201.
118 Alexandridis, P., Athanassiou, V., Fukuda, S. and Hatton, T. A. 1994. Surface-activity of poly(ethylene oxide)-block-poly(propylene oxide)-block-poly(ethylene oxide) copolymers. Langmuir 10(8):2604-2612.
119 Munoz, M. G., Monroy, F., Ortega, F., Rubio, R. G. and Langevin, D. 2000. Monolayers of symmetric triblock copolymers at the air-water interface. 2. Adsorption kinetics. Langmuir 16(3):1094-1101.
120 Peters, T. J. 1995. All about albumin: Biochemistry, genetics and medical applications. ed.: Academic Press.
121 Shen, J. J. S. and Probstein, R. F. 1977. Prediction of limiting flux in laminar ultrafiltration of macromolecular solutions. Ind. Eng. Chem. Fundam. 16(4):459-465.
122 Gordon, M. and Taylor, J. S. 1952. Ideal copolymers and the second.order transitions of synthetic rubbers. I. Non-crystalline copolymers. J. Appl. Chem. 2:493-500.
123 Hassan, H. M. and Mumford, C. J. 1993. Mechanisms of Drying of Skin-Forming Materials. 3. Droplets of Natural Products. Dry. Technol. 11(7):1765-1782.
124 Albertsson, P. A. 1986. Partion of cell particles and macromolecules. 3rd ed., New York: John Wiley & Sons, Inc.
125 Flory, P. J. 1953. Principles of Polymer Chemistry. ed., Itacha, NY: Cornell University Press.
126 Heller, M. C., Carpenter, J. F. and Randolph, T. W. 1997. Manipulation of lyophilized-induced phase separation: implications for pharmaceutical proteins. Biotechnol. Prog. 13:590-596.
127 Forciniti, D., Hall, C. K. and Kula, M. R. 1990. Interfacial tension of polyethyleneglycol-dextran-water systems: influence of temperature and polymer molecular weight. J. Biotech. 16(3-4):279-296.
128 Benjamins, J. and Lucassen-Reynders, E. H. 1998. Surface dilatational theology of proteins adsorbed at air/water and oil/water interfaces. In Miller, R., editor Proteins at liquid interfaces, ed., Amsterdam: Elsevier. p 341-284.
129 Pereira, L. G. C., Theodoly, O., Blanch, H. W. and Radke, C. J. 2003. Dilatational rheology of BSA conformers at the air/water interface. Langmuir 19:2349-2356.
130 Barrett, D. A., Hartshorne, M. S., Hussain, M. A., Shaw, P. N. and Davies, M. C. 2001. Resistance to nonspecific protein adsorption by poly(vinyl alcohol) thin films adsorbed to a poly(styrene) support

matrix studied using surface plasmon resonance. Analytical Chemistry 73(21):5232-5239.
131 Munoz, M. G., Monroy, F., Ortega, F., Rubio, R. G. and Langevin, D. 2000. Monolayers of symmetric triblock copolymers at the air-water interface. 1. Equilibrium properties. Langmuir 16(3):1083-1093.
132 Avranas, A. and Iliou, P. 2003. Interaction between hydroxypropylmethylcellulose and the anionic surfactants hexane-, octane-, and decasulfonic acid sodium salts, as studied by dynamic surface tension. J. Colloid Interface Sci. 258:102-109.
133 Fäldt, P. 1995. Surface composition of spray-dried emulsions. Ph.D. Thesis. Lund University. Lund.
134 Arboleya, J.-C. and Wilde, P. J. 2005. Competitive adsorption of proteins with methylcellulose and hydroxypropyl methylcellulose. Food Colloids 19:485-491.
135 Hickey, A. J., Concessio, N. M., Van Oort, M. M. and M., P. R. 1994. Factors Influencing the Dispersion of Dry Powders as Aerosols. Pharm. Technol.:58-64.
136 Stubberud, L. and Forbes, R. T. 1998. The use of gravimetry for the study of the effect of additives on the moisture-induced recrystallisation of amorphous lactose. Int. J. Pharm. 163(1-2):145-156.
137 Corrigan, D. O., Healy, A. M. and Corrigan, O. I. 2002. The effect of spray drying solutions of polyethylene glycol (PEG) and lactose/PEG on their physicochemical properties. Int. J. Pharm. 235(1-2):193-205.
138 Berggren, J. and Alderborn, G. 2004. Long-term stabilisation potential of poly(vinylpyrrolidone) for amorphous lactose in spray-dried composites. Eur. J. Pharm. Sci. 21(2-3):209-215.
139 Maa, Y. F., Costantino, H. R., Nguyen, P. A. and Hsu, C. C. 1997. The effect of operating and formulation variables on the morphology of spray-dried protein particles. Pharm. Dev. Tech. 2:213-223.

Acta Universitatis Upsaliensis

Digital Comprehensive Summaries of Uppsala Dissertations from the Faculty of Pharmacy 15

Editor: The Dean of the Faculty of Pharmacy

A doctoral dissertation from the Faculty of Pharmacy, Uppsala University, is usually a summary of a number of papers. A few copies of the complete dissertation are kept at major Swedish research libraries, while the summary alone is distributed internationally through the series Digital Comprehensive Summaries of Uppsala Dissertations from the Faculty of Pharmacy. (Prior to January, 2005, the series was published under the title "Comprehensive Summaries of Uppsala Dissertations from the Faculty of Pharmacy".)

Distribution: publications.uu.se
urn:nbn:se:uu:diva-5904

ACTA
UNIVERSITATIS
UPSALIENSIS
UPPSALA
2005